EKL-7 is a putative MPK-1 ERK target during *C. elegans* excretory duct cell fate specification

Preston Chin

A thesis submitted to McGill in partial

fulfillment of the requirements of the degree of

Master of Science

Department of Anatomy and Cell Biology

McGill University, Montréal, Quebec

August 2015

Acknowledgements

I would like to wholeheartedly thank my supervisor, Dr. Christian Rocheleau, for his continual guidance, encouragement, and understanding throughout my Masters studies in the Department of Anatomy and Cell Biology at McGill. I received nothing but compassionate support since I joined his lab as a graduate student. I would also like to express gratitude towards all the members of the Rocheleau lab for always being available to give help when needed and above all, thank them for their lasting friendship. In particular, I would like to thank Jung Hwa Seo for providing assistance on many of the methods mentioned in this paper. Lastly, I would like to thank Dr. Meera Sundaram at the University of Pennsylvania for sharing unpublished data and providing the strain UP2883 to aid this project.

Table of Contents

Table of Contents

List of Figures

List of Tables

Abstract

The Ras/Mitogen-Activated Protein Kinase (MAPK) signalling pathway regulates multiple developmental events including the determination of the excretory duct cell fate (EDC) and its maintenance. A lack of an EDC causes a phenotypically distinct rod-like lethality due to an inability to excrete waste fluids. The scaffolding proteins Kinase Suppressor of Ras (KSR), KSR-1 and KSR-2, are redundantly required for Ras/MAPK signalling and specification of the EDC. *ksr-1(n2526)* null mutants exhibit a wild-type phenotype, but are sensitive to any mutations that reduce Ras/MAPK signalling. Subsequently, a forward genetic screen identified *vh20* as a candidate allele for Y39G10AR. 7, which I have since named *ekl-7* as an enhancer of *ksr-1* lethality *(*ekl). *ekl-7(vh20); ksr-1(n2526)* double mutants reveal a penetrance of rod-like lethality of 35%. The *vh20* E422K missense mutation disrupts a C-terminal negatively charged domain. EKL-7 is a *Caenorhabditis*-specific protein. However, protein alignments identified a cluster of consensus ERK phosphorylation sites (PX-S/T-P or S/T-P) and ERK docking sites (FXFP and D domain) similar to those found in MPK-1 ERK targets LIN-1 and EOR-1. I hypothesize that EKL-7 is a novel downstream target of MPK-1 ERK that promotes the EDC fate or its maintenance. To characterize the rod-like lethality of *ekl-7(vh20); ksr-1(n2526)* mutants, I generated animals carrying an EDC and apical junction marker. While *ekl-7(vh20)* single mutants are essentially wild-type, *ekl-7(vh20); ksr-1(n2526)* mutants have EDCs that fail to properly autofuse into a seamless toroidal cell due to a failure to express *aff-1*, a cell surface protein required for autofusion. This suggests that EKL-7 might have a specific role in EDC autofusion during its specification. To elucidate how *ekl-7(vh20)* functions within the Ras/MAPK signalling pathway, I have generated double mutants with *lin-1* and *eor-1* on the basis that these transcriptional regulators function downstream of MPK-1 ERK and have demonstrated synergistic effects during EDC fate specification. I have observed that both *ekl-7(vh20); lin-1(n2515)* and *ekl-7(vh20); eor-1(cs28)* doubles display enhanced rod-like lethality, suggesting that EKL-7 functions in parallel to LIN-1 and EOR-1. As well, *ekl-7(vh20); lin-1(n2515)* and *ekl-7(vh20); eor-1(cs28)* mutants show various defects in their excretory systems. The ability of the Ras/MAPK pathway to regulate so many developmental processes likely depends on the suite of downstream MPK-1 ERK targets available in a given cell type. EKL-7 might define an important specificity factor that functions in coordination with LIN-1 and EOR-1 to promote the EDC fate and its maintenance as opposed to promoting other cellular processes regulated by Ras/MAPK signalling.

Abrégé

La Ras/Protèine Kinase Activée par des Mitogènes (MAPK) voie de signalisation régule beaucoup d'événements de développement, y compris la détermination du sort de la cellule de canal excréteur (EDC) et de son entretien. Un manque d'une EDC provoque une létalité de tige phénotypiquement distincte en raison d'une incapacité à excréter les déchets liquides. Le protéines d'échafaudage kinase suppresseur de Ras (KSR), KSR-1 et KSR-2, sont redondante nécessaire pour Ras/MAPK signalisation et la spécification de la EDC. *ksr-1(2526)* mutants nuls présentent un phénotype de type sauvage, mais ils sont sensibles à des mutations qui réduisent la signalisation Ras/MAPK. Par la suite, un écran génétique identifiée *vh20* comme un allèle candidat pour *Y39G10AR.7*, que j'ai appelé depuis *ekl-7* comme un activateur de *ksr-1* létalité (*ekl*). Les *ekl-7(vh20); ksr-1(2526)* doubles mutants ont une fréquence de létalité de tige de 35%. Le *vh20* E422K mutation faux-sens perturbe un domaine chargé négativement C-terminale. EKL-7 est une protéine spécifique à Caenorhabditis. Mais, les alignements de protéines ont identifié un groupe de consensus sites de phosphorylation ERK (PX-S/T-P et S/T-P) et les sites d'accueil ERK (FXFP et D domaine) similaire à ceux trouvés dans LIN-1 et EOR-1, les substrats en aval de MPK-1 ERK. Je hypothèse que EKL-7 est un nouveau substrat en aval de MPK-1 ERK qui régule positivement le sort EDC ou son entretien. Pour caractériser la létalité de tige des mutants de *ekl-7(vh20); ksr-1(n2526)*, j'ai généré des animaux portant une marque de la EDC et jonction apicale. Alors que les mutants *ekl-7(vh20)* sont essentiellement de type sauvage, les mutants *ekl-7(vh20); ksr-1(n2526)* ont les EDCs qui ne autofuse correctement dans une cellule toroïdal sans soudure en raison d'une panne d'exprimer *aff-1*, une protéine fusogène nécessaire pour autofusion. Ceci suggère que EKL-7 pourrait avoir un rôle spécifique dans EDC autofusion lors de sa spécification. Pour élucider la façon common *ekl-7(vh20)* fonctions au sein de la voie de signalisation Ras/MAPK, j'ai produit des doubles mutants avec *lin-1* ou *eor-1* parce que ces régulateurs de transcription fonctionnent en aval de MPK-1 ERK et ont démontré des effets synergiques lors de la spécification du sort EDC. J'ai observé que les deux mutants, *ekl-7(vh20); lin-1(n2515)* et *ekl-7(vh20); eor-1(cs28)* démontrent améliorée létalité en forme de tige, ce qui suggère que EKL-7 fonctionne en parallèle à LIN-1 et EOR-1. En plus, *ekl-7(vh20); lin-1(n2515)* et *ekl-7(vh20); eor-1(cs28)* mutants montrent divers défauts dans leurs systèmes excréteurs. La capacité de la voie Ras/MAPK pour réguler de nombreux processus de développement dépend probablement à la suite de substrats en aval de MPK-1 ERK qui sont disponibles dans un type de cellule spécifique. EKL-7 pourrait être une spécificité de facteur important qui fonctionne en coordination avec LIN-1 et EOR-1 pour réguler positivement le sort EDC et de son entretien, par opposition à la promotion d'autres processus cellulaires régulés par de signalisation Ras/MAPK.

Introduction

C. elegans as a model organism

Caenorhabditis elegans (*C. elegans*) is a non-parasitic, semi-transparent nematode that is widely used as a genetic tool to study several essential cellular processes like cell growth, signalling, differentiation, metabolism, division, and apoptosis. As a model organism, *C. elegans* have many characteristics that make them particularly amenable for genetic study.

Firstly, *C. elegans* are found as either as self-fertilizing hermaphrodites or males, specified by a particular individual's X chromosome to autosome ratio [1]. This offers many advantages for genetic manipulation and study. Since hermaphrodites reproduce by self-fertilization, all or most their progeny will be genetically identical. As well, recessive mutations will segregate according to Mendelian rules with each generation of selfing, allowing those mutations to be isolated [2]. Lastly, genetic material can be exchanged between individuals if a hermaphrodite is fertilized with male sperm. Therefore, crosses between hermaphrodites and males can be designed to produce progeny with virtually any desired genotype.

The entire somatic cell lineage for a wild-type *C. elegans* is invariant and has been mapped, starting from a single somatic cell to a final ~1000 somatic cells in the adult [3]. Furthermore, cell divisions and positions during development are stereotyped. Owing to the transparency of the animal, individual cells can therefore be tracked visually using simple light microscopy, allowing study of the effects of specific genes on events like cell migration or fate determination.

C. elegans have many attributes that make them particularly easy to maintain and store for experimental use. A single self-fertilizing hermaphrodite can produce around 350 progeny and will produce even more if fertilized by a male's sperm [4], meaning a large number of animals will always be available for study. *C. elegans* may be maintained on agar plates with a diet of bacterium *Escherichia coli* (*E. coli*). Their small size (~1mm) allows several thousands of animals to be grown on a single plate. Animals may be frozen and stored at -80^{o}C for several years and thawed whenever needed. Finally, the experimental cycle for *C. elegans* is relatively short since the time between each generation of animals is typically around 3 to 4 days [5].

Life Cycle of *C. elegans*

The life cycle of *C. elegans* consists of an embryonic stage, four larval stages (L1-L4), and adulthood (Figure 1). Embryogenesis begins after fertilization and consists of two broad stages: cell proliferation and organogenesis/morphogenesis [6]. The first 150 minutes of proliferation takes place *in utero* until the embryo is laid outside at the 30-cell stage. During the next 200 minutes, the majority of cell divisions occur resulting in a large number of cell rearrangements due to shuffling [7]. Further cell rearrangements occur during the gastrula stage, during which cells will make specific cell migrations while increasing in cell number [8]. Proliferation ends with a roughly spherical embryo with three defined germ layers. Organogenesis/morphogenesis involves terminal cell differentiation without any further cell divisions, resulting in the formation of tissues and organs. During this time, the embryo elongates extensively and the main body plan of the adult animal is fully established.

Post-embryonic development begins approximately 3 hours after the hatched larva feeds if food is immediately available [9]. The animal will enter the first of four larval stages, L1, and progress through each subsequent stage until adulthood. Each larval stage is separated by a period of inactivity when a new cuticle that surrounds the animal is made and the old cuticle is molted [10]. If the environment is unfavourable for development, L2 larvae may enter a stage of survival known as the "dauer" stage. Poor environmental conditions include a lack of food or exceedingly high temperatures. During the dauer stage, larvae produce a more resilient cuticle that encompasses the whole animal, become thinner in appearance, and will stop feeding entirely [11]. Dauer larvae may survive for months on end without feeding and are therefore the most commonly found form in nature. Animals will exit the dauer stage once in the presence of food and will proceed to the L4 larval stage after about 10 hours [11]. Once adults, animals will produce embryos for another 4 days. During post-embryonic development, Receptor Tyrosine Kinase (RTK)/Ras/Mitogen-Activated Protein Kinase (MAPK) signalling is used repeatedly to mediate several cell specifications and migrations in various organ systems.

Canonical RTK/Ras/MAPK signalling pathway

The Receptor Tyrosine Kinase (RTK)/Ras/Mitogen-Activated Protein Kinase (MAPK) signalling pathway is an evolutionarily conserved signalling pathway that is used repeatedly during animal development to regulate cellular processes like cell proliferation, differentiation, metabolism, and apoptosis. [12] Expectedly, mutations in core components of this pathway are well characterized in numerous cases of human cancer [13][14] and developmental syndromes like non-obese diabetes [15] or neurofibromatosis [16].

Receptor tyrosine kinases are a large family of Type I cell surface receptors that consist of a large extracellular ligand-binding domain, a single-pass transmembrane domain, and a cytoplasmic tail including a conserved protein tyrosine kinase domain (PTK) [17]. Types of RTKs include epidermal growth factor receptor (EGFR), fibroblast growth factor receptor (FGFR), insulin receptor, and vascular endothelial growth factor receptors (VEGFR) [18].

Binding of a ligand to the extracellular domain of an inactive RTK will typically cause receptor dimerization, stimulating intrinsic protein tyrosine kinase activity to cause trans-autophosphorylation of intracellular tyrosine residues on both cytoplasmic tails [19][20] (Figure 2). These phosphotyrosine residues act as binding sites for any adaptor proteins with Src Homology 2 (SH2) or phosphotyrosine binding (PTB) domains like GRB2 [21]. Once associated with these phosphotyrosines, GRB2 adaptor protein recruits Son of Sevenless (SOS) by its proline-rich domains and brings SOS into close proximity to Ras, a small GTPase located

on the peripheral membrane [13] SOS is a guanine nucleotide exchange factor for Ras and promotes dissociation of GDP from an inactive Ras, allowing for Ras to bind any available GTP and become activated [22]. Activated Ras then recruits Raf kinases to the plasma membrane which is believed to cause conformational changes that result in its activation and stimulation of its serine/threonine kinase activity [23]. Active Raf then activates MAPK/ERK kinase (MEK) by phosphorylating specific serine and threonine residues, which itself phosphorylates and activates Extracellular Regulated Kinase (ERK) [24]. Once activated, ERK phosphorylates hundreds of known substrates, many of which are localized to the nucleus and regulate transcription of genes [24]. It is through this pathway that an extracellular ligand can trigger specific biological changes within the cell.

RTK/Ras/MAPK Signalling in *C. elegans*

Studies in *C. elegans* have been massively insightful towards how canonical aspects of Ras signalling function and are regulated. LET-60/Ras is known to function downstream of two RTKs: LET-23/EGFR and EGL-15/FGFR (Figure 2). In *C. elegans*, Ras/MAPK signalling involves the same core machinery but is not required for cell proliferation and instead controls numerous developmental biological processes. Activation of LET-23/EGFR by LIN-3/EGF ligand and stimulates a MAPK cascade with kinases LIN-45/Raf, MEK-2/MEK, and MPK-1/ ERK which regulates specification of vulval cell, excretory duct cell (EDC), and P12 ectoblast fates [25]. EGL-15/FGFR is activated by two ligands, EGL-17/FGF and LET-756/FGF and has functions in sex myoblast migration [26], sex muscle differentiation [27], axon outgrowth [28], and fluid homeostasis [29].

Scaffolding Proteins and KSR

Scaffolding proteins are amongst the key regulators of Ras/MAPK signalling and mediate assembly of multiprotein signalling complexes by bringing effectors into close proximity to their substrates, shielding kinases from deactivating phosphatases, and even integrating crosstalk from other pathways [30][31]. These scaffolds also modulate the spatiotemporal aspects of signalling and target signalling complexes to specific subcellular localizations [32][33]. Overall, scaffolding proteins have an essential role in providing specificity to outputs of Ras/MAPK signalling.

One well studied scaffolding protein involved with Ras/MAPK signalling is Kinase Suppressor of Ras (KSR), which was originally identified as a positive regulator of Ras/MAPK signalling in genetic screens in *Drosophila melanogaster* and *C. elegans* [34]. KSR scaffold proteins have five conserved domains: an N-terminal KSR-unique domain (CA1), a proline-rich domain (CA2) a cysteine-rich zinc-finger domain (CA3), a serine/threonine rich domain (CA4), and a C-terminal putative kinase domain (CA5) [35] (Figure 3). The presence of the C-terminal kinase domain has been the cause of a longstanding debate on whether KSR functions primarily as a scaffold or a kinase. However, most evidence support the idea that KSR functions independently of any kinase activity. KSR was found to directly interact with both MEK-1 and MEK-2 by its CA5 domain [36]. It was shown that ERK also binds directly to its CA4 which contains a consensus FXFP docking motif, an interaction that only occurs upon activation of Ras/MAPK signalling [37]. Studies have shown that kinase-dead mutants of KSR were also able to complement *ksr* null mutants in *C. elegans*, further supporting that its biological function is

primarily as a scaffolding protein [38]. Nevertheless, the fact that KSR is capable of recruiting several bonafide kinases like Raf, MEK, and ERK, has made it difficult to discern whether it does have unique functions in Ras/MAPK signalling as a kinase.

In *C. elegans*, KSR is encoded by two paralogs, *ksr-1* and *ksr-2*, that are redundantly required for specification of the vulval cell and EDC fates [39][40]. Since the excretory system in *C. elegans* has an essential function in osmoregulation and excretion of excess body waste fluids, animals that fail to specify an EDC fill up with their own waste, become turgid, and die of a phenotypically distinct rod-like lethality during early larval development [41][42][43]. Mutants that lack both *ksr-1* and *ksr-2* are completely inviable which indicates a functional redundancy between the two. As such, *ksr-1* null mutants are essentially wild-type, but are sensitive to mutations that reduce Ras signalling further which provides a useful sensitized background to identify novel regulators of Ras/MAPK signalling [44]. Interestingly, *ksr-1* and *ksr-2* have also been reported to have unique roles in Ras/MAPK signalling: *ksr-1* regulates sex myoblast migration and *ksr-2* regulates meiotic progression in the germline [40].

Ras/MAPK signalling and development in *C. elegans*

Vulval development

Development of the vulva in a hermaphroditic *C. elegans* occurs during post-embryonic development. In the adult, the vulva physically connects the uterus to the exterior of the animal and functions as part of the egg-laying apparatus of the animal. This organ system has been used as an important model for studying EGFR/Ras/MAPK, its role in organogenesis and tissue remodelling, and its regulation by other signalling pathways like the Notch/LIN-12 pathway.

Vulval development begins with the generation of eleven epidermal precursors during the L1 larval stage that are born from ventral neuro-ectoblasts (P1-P11) [3] as their posterior daughters, and are accordingly named P1.p, P2.p,..., P11.p. WNT/β-catenin signalling act through Hox genes, including *lin-39*, to cause six of those cells, P3.p - P8.p, to resume a competent state and remain responsive to developmental signals for the vulval cell fate [45]. Cell ablation experiments have demonstrated that all six vulval precursor cells (VPCs), P3.p to P8.p, form an equivalence group that each have the potential to generate vulval cells [46][47][48], but in normal cases, the vulval cell fate is restricted to the three central VPCs due to the simultaneous regulation by several intercellular signalling pathways (Figure 4). A LIN-3/EGF inductive signal produced by the anchor cell activates LET-23/EGFR in P5.p, P6.p, and P7.p, but P6.p receives the strongest signal and immediately adopts a primary (1º) vulval cell fate [49]. Concurrently, a lateral LIN-12/Notch ligand is produced between induced VPCs and specifies the secondary (2º) vulval cell fate, but cross inhibition between the two signalling pathways ensures that only P5.p

and P7.p adopt the 2º vulval cell fate; LET-23/EGFR activation upregulates LIN-12/Notch ligand production and downregulates LIN-12/Notch receptor expression in the P6.p while LIN-12/ Notch receptor activation in P5.p and P7.p inhibits LET-23 signalling [50][51][52]. All the remaining uninduced VPCs (P3.p, P4.p, and P8.p) adopt tertiary (3º) cell fates and irreversibly fuse with the Hyp7 epidermis [53]. Ablation of the anchor cell before the L3 larval stage results in all the cells adopting 3º cell fates, demonstrating that the anchor cell's LIN-3/EGF signal is necessary for the 1º and 2º vulval cell fates [46].

Mutations affecting genes responsible for proper vulval development cause many observable defects. Animals that have mutations that reduce Ras signalling will often have defects in vulval induction, resulting in a vulvaless (Vul) phenotype. Vul mutants are unable to lay eggs such that they hatch internally and must eventually leave by physically breaking free from the corpse of the mother [54]. Animals with gain-of-function mutations in Ras signalling will often result in a multivulva (Muv) phenotype. Muv mutants usually have additional vulval protrusions known as pseudovulva due to over-induction of vulval cells that surround a functional vulva [55].

Excretory duct development

Ras/MAPK signalling also plays an important role in development of the excretory system in *C. elegans*, which functions analogously to a higher order renal system in osmoregulation and the collection and elimination of waste fluids [56][57]. Located at the ventral midline near the terminal pharyngeal bulb, the system is comprised of four cells of the AB cell lineage: a pore cell, an excretory duct cell (EDC), a canal or excretory cell, and a pair of fused gland cells [6].

This system makes an extensive number of epithelial cell junctions with its surroundings and between its cell constituents. The canal cell, EDC, and pore cell all form gap junctions with one another, and the bilateral canals originating from the canal cell that extend throughout the length of the animal form gap junctions with the hypodermis [58]. As well, adherens junctions are formed at many points to seal off the excretory system. Namely, the region where the canal cell, gland cells, and EDC meet one another at a three-way intercellular junction known as the secretory-excretory junction, between the EDC and pore cell, the autocellular junction of the pore cell that it forms when wrapping around the duct on to itself, and the region where the pore cell meets the Hyp7 epidermis [59]. The excretory duct in *C. elegans* offers a simple model to study the effects of Ras signalling on cell morphogenesis, epithelial junction remodelling, cell migration, and cell fate specification (Figure 5).

The epithelial progenitors for the canal cell, EDC and pore cell (known as the G1 pore cell during early embryogenesis) are born in different areas of the developing embryo (Figure 5). The canal cell is known to be the source of the LIN-3/EGF inductive signal that promotes the EDC fate in the initially equivalent presumptive EDC and G1 pore cells [60]. Both the EDC and G1 pore are competent for the EDC fate and compete for the most proximal position to the canal cell as they move to the ventral midline during ventral enclosure [41][6]. However, it is believed that the left-biased asymmetric position of the EDC progenitor provides it a competitive advantage and it therefore reaches and adheres to the canal cell first, resulting in the G1 pore progenitor taking on a ventral position. Once meeting one another, the tandemly-linked cells wrap around themselves to form autocellular junctions, but only the G1 pore maintains this junction and

instead the EDC autofuses into a seamless toroid. Ras/MAPK signalling has been shown to have a role in many aspects of EDC versus G1 pore cell identity at this point: expression of EDC-specific factors like *lin-48*, the autofusion event, and maintenance of epithelial junctions with the surrounding cells. It is thought that some unknown lateral signal between the EDC and pore also restricts the EDC cell fate to one progenitor once it has fully committed to that fate. When the embryo has reached the 1.5-fold stage, the excretory system consists of tandemly-linked unicellular tubes that share a common lumen [60]. The EDC and canal cell then undergo further morphogenesis and elongation until the excretory system is fully functional upon hatching and entry into the L1 larval stage. Curiously, the system then undergoes additional remodelling, and the G1 pore withdraws dorsally from the system and is replaced by a nearby epidermal cell, G2, which concurrently wraps around the duct and forms an autocellular junction. The G2 cell then further divides during the L2 stage to produce a neuronal (G2.a) and epithelial (G2.p) daughter that will function as the pore cell for the rest of the animal's life. Evidently, there is an extensive amount of epithelial junction remodelling that must occur during this time. Use of *sos*-1 temperature sensitive mutants demonstrated a requirement for Ras/MAPK signalling beyond cell fate specification up until the L2 larval stage, indicating that the pathway may be needed for other aspects of excretory duct development or maintenance [60].

AFF-1

aff-1 encodes a cell surface protein that is responsible for numerous specific cell fusion events in *C. elegans* and is thus known as a fusogen [61][62][63]. These include fusion of the anchor cell in the vulval system and lateral seam cells of the hypodermis. Therefore, a forward genetic screen was performed for mutants with an egg laying defective (Egl) phenotype due specifically to defects in anchor cell invasion which lead to the identification of *aff-1* [62]. *aff-1* expression appears to be regulated in a cell-specific manner: in the anchor cell, *aff-1* is regulated by FOS-1 transcription factor, while in the lateral seam cells, *aff-1* expression is stimulated by LIN-29 zinc-finger transcription factor [62][64]. *aff-1* also has been reported to have a role in autofusion of the EDC as *aff-1* mutants have an EDC that maintain its autocellular junction. It is not yet known how *aff-1* expression is regulated in the EDC.

Since Ras/MAPK signalling promotes the EDC fate over the G1 pore fate in two initially equivalent epithelial progenitors, defects in Ras signalling often result in distinct cell fate transformations. In mutants where Ras signalling is sufficiently reduced, neither cell will be able to take on the EDC fate, resulting in a 2 G1 pore cell: 0 EDC phenotype. The EDC progenitor that failed to be induced adopts characteristics of a G1 pore cell including maintenance of its autocellular junction and a failure to express duct-cell specific *lin-48*. In mutants where Ras signalling is overstimulated, the G1 pore cell progenitor is induced to become an EDC and takes on characteristics of an EDC-like cell, including a failure to maintain its autocellular junction and expression of duct-cell specific marker *lin-48* [60].

Downstream ERK substrates, LIN-1 and EOR-1

The ability for the EGFR/Ras/MAPK signalling pathway to regulate so many different, sometimes even opposing, biological processes likely depends on the cumulative regulation by the plethora of downstream regulators in the pathway. A central regulator of signalling outputs is MPK-1/ERK, which alone has been found to target and activate numerous substrates to elicit tissue-specific responses [65]. Therefore, how MPK-1/ERK controls aspects downstream of Ras signalling is integral to our understanding of how Ras signalling may be used repeatedly during animal development. In *C. elegans*, two transcription factors, LIN-1 and EOR-1, are MPK-1/ERK substrates that have been extensively studied.

LIN-1/ETS-domain-containing transcription

lin-1 encodes a 441 amino acid ETS-domain-containing transcription factor that is homologous to members of the ETS gene subfamily that includes human ELK-1, -3, and -4 [66] and is an important general effector of EGFR/Ras/MAPK signalling pathway regulated by MPK-1/ERK (Figure 6A). In humans, ETS transcription factors also function downstream of Ras/ERK signalling. In *C. elegans*, LIN-1 appears to have positive and negative roles in Ras-dependent specification of several cell fates during development of the vulva, the excretory duct, the male tail, and anterior-posterior patterning of the posterior ectoderm [67][68][4]. With regards to its role as a regulator of vulval patterning, it is an inhibitor of the 1º vulval cell fate that is normally negatively regulated by Ras signalling [54]. Its functionality has been shown to be dependent on its ETS domain (GGAA/T) as *lin-1* loss-of-function *(lf)* alleles that affect this domain cause a strong Muv phenotype. ETS domains are reported to have a winged helix-loop-helix structure

that conforms to the major groove of DNA and makes contact with the DNA phosphate backbone [69]. A genetic screen identified many *lin-1(gf)* mutants that had constitutively active LIN-1 that was unresponsive to negative regulation by Ras/ERK signalling, all of which had a point mutation in a FQFP motif located in the C-terminal side of LIN-1 [70] (Figure 6A). This FQFP motif conforms to the consensus motif of one well characterized ERK docking site, FXFP [71], and is a necessary site also found on ETS protein ELK-1 [72] (Figure 6B). Another known ERK docking site present on LIN-1 is the D domain motif which is also found on ELK-1. In a separate screen, it was reported that in one particular gain-of-function mutant, *lin-1(cs50)*, a Ser315 located in one of 18 potential ERK phosphorylation sites present on LIN-1 was required for its downregulation [60][73] (Figure 6A). Therefore, these data strongly suggest *lin-1 is* regulated by phosphorylation by MPK-1/ERK. More recently, biochemical studies using a yeast two-hybrid system have demonstrated that SUMOylation of the N-terminal end of LIN-1 can recruit many known components of the nucleosome remodelling and histone deacetylation (NuRD) transcriptional repression complex like RAD-26 and EGL-27, both which are known inhibitors of vulval cell fates in *C. elegans* [74]. With regards to development of the excretory duct, less is known how LIN-1 is regulated, but LIN-1 also appears to be a negative regulator of the EDC fate. *lin-1(gf)* mutants have low penetrance of rod-like lethality in L1 larva, while *lin-1(lf)* mutants often show specification of two EDCs and expression of *lin-48* in an EDC-like cell instead of specification of a G1 pore cell [75].

A long-established question involving *lin-1* is how it is able to elicit tissue-specific effects on development. So far it has been reported that during vulval development, LIN-1 associates with

LIN-31, a member of the winged-helix family of transcription factors that is restricted to vulval cells [76] and forms a heterodimer that inhibits vulval induction [77]. Upon stimulation of Ras signalling, LIN-1 and LIN-31 are phosphorylated by MPK-1/ERK which disrupts the heterodimer, effectively relieving inhibition on vulval cell fate specification [68]. A possibility is that LIN-1 is regulated in other tissues by a similar mechanism of tissue-specific interaction. Nearly all studies that have concerned LIN-1 support the idea that its phosphorylation state is integral to its regulation [73][74][75].

EOR-1/PLZF transcription factor

eor-1 encodes an ortholog of human PLZF, a BTB/zinc-finger transcription factor [78] that was initially identified in an screen for enhancers of *lin-45* Raf-dependent Vul, egg-laying (Egl) and excretory system defects [73]. Loss-of-function alleles of *eor-1* in this screen demonstrated that *eor-1* alone has a weak positive role in excretory development and vulval development, indicated by a low penetrance of rod-like lethality and Egl phenotypes. Interestingly, despite the Egl phenotype, which would indicate an effect on vulval development, loss of *eor-1* resulted in no effect on vulval induction so the basis of this vulval phenotype remained unclear [73]. Regardless, it was proposed that *eor-1* may have different requirements in different tissues. Structurally, EOR-1 is similar to PLZF: it contains an N-terminal BTB domain and nine C2H2 zinc-finger domains that each consist of a beta hairpin and alpha helix (β-β-α) [79] structure that is known to be able to bind the major groove of DNA [80] (Figure 7A and B). Consistent with its role as a general regulator of gene expression across many tissues, GFP::EOR-1 constructs showed that it is widely expressed in cells during development and is nuclear-localized [78]. It

has been reported that EOR-1 is an *in vitro* ERK substrate that is dependent on its BTB domain for phosphorylation [81], a finding that is consistent with epistasis experiments that place *eor-1* genetically downstream of MPK-1/ERK [78]. What remains unclear is whether EOR-1 functions as a transcriptional activator or repressor in Ras/MAPK signalling.

Synergistic function between LIN-1 and EOR-1

Interestingly, mutations in *lin-1* and *eor-1* have demonstrated synergistic interactions during both vulval and excretory tube development. With regards to vulval development, *lin-1(n304); eor-1(cs28)* double loss-of-function mutants born from heterozygote mothers (and therefore are maternally rescued) are reported to have mixed Vul and Muv phenotypes in the same animal, where all the VPCs stochastically adopt vulval or non-vulval fates [78]. In terms of excretory system development, while individually *lin-1(n304)* and *eor-1(cs28)* mutants show little to no penetrance of rod-like lethality, *lin-1(n304); eor-1(cs28)* double mutants are entirely inviable due to fully penetrant rod-like lethality [78] associated with a failure to properly specify an EDC [60]. Altogether, these studies support the idea that somehow *lin-1* switches its apparent role as a negative regulator and behaves as a positive regulator of the EDC and vulval cell fates when placed in the *eor-1(lf)* background. This cryptic relationship suggests that somehow *lin-1* and *eor-1* might cooperate with each other in a tissue-specific manner.

Y39G10AR.7 is identified as an *ekl* and a putative ERK substrate

As mentioned earlier, *ksr-1* null mutants are wild-type but are sensitive to any further reductions in Ras signalling. A forward mutagenesis screen for enhancers of *ksr-1* lethality (*ekl*) identified one mutation, *vh20*, as having a penetrance of rod-like lethality of 31%. Chromosomal mapping using single-nucleotide polymorphisms (SNPs) and interval mapping placed *vh20* on the left arm of chromosome I in a 6 map unit region between SNPs I: -12 (Y71G12A) and I: -6 (W03D8) [82]. This particular region of chromosome I lacks any genes currently known to be associated with the Ras/MAPK pathway, so *vh20* was proposed to be a novel Ras regulator. Subsequent whole genome sequencing identified *vh20* as a missense allele involving a change from a conserved Glutamic acid to a Lysine residue (E422K) within a span of negatively charged residues in a candidate gene, *Y39G10AR.7* [J.H. Seo and C.E.R., unpublished]. Protein alignments with the protein sequence of Y39G10AR.7 reveal a cluster of conserved ERK phosphorylation sites (PX-S/T-P or S/T-P) and ERK docking sites (D domain and FXFP motifs) that strongly suggest that Y39G10AR.7 is a novel ERK substrate (Figure 8). Incidentally, this gene had been identified previously in a genome-wide RNAi screen for *ekl* genes but remained unpublished due to low penetrance of the phenotype [Y. Berenstein, M. Sundaram and C.E.R., unpublished][44]. Y39G10AR.7 does not have a clear homolog outside of the *Caenorhabditis* genus according to its protein sequence. Since *Y39G10AR.7* appeared in two separate screens for enhancers of *ksr-1* lethality and was a good contender to be a novel ERK substrate, I hypothesized it had a potential role in specification of the EDC fate and named the gene *ekl-7*.

The goal of my Masters thesis was to characterize the underlying excretory duct defect that may be related to rod-like lethality observed in *ekl-7(vh20); ksr-1(n2526)* mutants, determine the role of *ekl-7* in Ras/MAPK signalling and its relationship with other effectors of the pathway, and to begin characterizing the *vh20* allele. I found that *ekl-7(vh20); ksr-1(n2526)* mutants partially specify an EDC: while they properly express duct-cell specific *lin-48* in the EDC, they fail to express *aff-1* fusogen required for EDC autofusion. I also show that *ekl-7* functions in parallel to *lin-1* and *eor-1* during specification of the EDC. I have yet to be determine if *vh20* is an allele for *Y39G10AR.7*, but my data are consistent with it being a hypomorphic allele. Altogether, I demonstrate EKL-7 functions as a positive regulator of Ras/MAPK signalling that may have a role as a specificity factor in conjunction with LIN-1 and EOR-1 during specification of the EDC.

Materials and Methods

Alleles and general maintenance

Maintenance, handling, and culturing of *C. elegans* were done using general methods as previously described [2]. All *C. elegans* strains described in this study used the wild-type parent var Bristol strain N2. Specific genes and alleles are described on Wormbase (www.wormbase.org) and many of the alleles listed below are available to order from the Caenorhabditis Genetics Center located in University of Minnesota, Minneapolis, MN. LG = linkage group.

LG I: *ekl-7(vh20)*

LG IV: *lin-1(n304), lin-1(n2515) dpy-13(e184), eor-1(cs28)*

LG X: *ksr-1(n2526)*

hT2[bli-4(e937) let-?(q782) qIs48]

jcIs1[AJM-1::GFP; rol-6(su1006)]

saIs14[plin-48::GFP]

ruIs32[ppie-1::GFP:H2B:pie-1 punc-119::unc-119(+)]

The strain UP2883 containing *csIs62(paff-1-NLS::GFP; grl-2::mRFP*] was kindly produced and provided by Meera Sundaram from the University of Pennsylvania, Philadelphia, PA.

Genetic manipulations and strain construction

Crosses were conducted on mating plates as previously described [83]. An hT2 genetic balancer was used for crosses that involved *ekl-7(vh20)* in order to ensure that the mutation was carried

forth in subsequent generations. Genetic balancers are either genetic constructs or chromosomal rearrangements that allow lethal mutations to be maintained stably in heterozygotes. This is especially useful when animals contain recessive lethal mutations that cannot be maintained as homozygotes due to inviability. Good balancers should have a number of traits: balanced heterozygotes should reveal phenotypes distinct from those of homozygotes, the balancer construct should be stable and not spontaneously 'unbalance' the mutation, and they should be able to be passed on through male sperm in order to be manipulated by genetic crosses. The hT2 GFP variant, hT2*[bli-4(e937) let-?(q782) qIs48]*, was chosen to balance *ekl-7* in this study because it balanced the appropriate region on chromosome I, contained an integrated pharyngeal GFP element, and is lethal when homozygous [84]

To generate *ekl-7(vh20); ksr(n2526); jcIs1[AJM-1::GFP; rol-6(su1006)]* transgenic double mutants, N2 ♂ were crossed with +/hT2 ⚥ to generate +/hT2 ♂. These +/hT2 ♂ were then crossed into *ekl-7; ksr-1* animals to generate *ekl-7/hT2; σ/ksr-1* ♂. Since *ksr-1* is located on the X chromosome, this strategy takes advantage of the fact that the *ksr-1* mutation must always be present in male progeny. These males were then mated with *ksr-1; jcIs1* ⚥ to generate +/*ekl-7; ksr-1; +/jcIs1* ⚥ progeny that could be identifiable by lack of GFP expression on the pharyngeal muscles and the roller (Rol) phenotype caused by expression of the transgene. These animals were then transferred to individual plates and maintained until rod-like lethality and expression of the *AJM-1* reporter was observed in all subsequent generations.

To generate *ekl-7(vh20); ksr-1(n2526); saIs14(plin-48::GFP]* transgenic double mutants, N2 ♂ were crossed with +/hT2 ♀ to generate +/hT2 ♂, which were crossed into *ksr-1; saIs14* ♀ to generate male progeny with the genotype, *+/hT2; σ/ksr-1; +/saIs14* ♂. These animals were then crossed with *ekl-7; ksr-1* ♀ to produce *ekl-7/hT2; ksr-1; +/saIs14* hermaphrodite progeny. GFP expression of the *saIs14* transgene was distinguishable from the GFP expression of the hT2 balancer because it also showed very specific expression near the anus. Animals were then transferred to individual plates, and animals with a non-green pharynx but green EDC were maintained.

To isolate *ekl-7(vh20)* single mutants, *ksr-1* was outcrossed by crossing *ekl-7; ksr-1* ♀ with *+/ hT2* ♂. *ekl-7/hT2; +/ksr-1* ♀ were selected out of the progeny and individually plated, and only those that produced progeny with no rod-like lethality were maintained.

To generate *ekl-7(vh20); saIs14[plin-48::GFP]* and *ekl-7(vh20); jcIs1[AJM-1::GFP; rol-6(su1006)]* transgenic single mutants, *ekl-7; ksr-1; saIs14* ♀ and *ekl-7; ksr-1; jcIs1* ♀ were crossed with *+/hT2* ♂ to generate *ekl-7/ hT2; +/ksr-1* ♀ heterozygous for each respective transgene. Progeny were then transferred to individual plates, and subsequence generations of non-green progeny that did not show any rod-like lethality but expressed each transgene were maintained.

To generate *ekl-7(vh20); eor-1(cs28)* double mutants, *eor-1* ♀ were crossed with *+/hT2* ♂ to generate *+/hT2; +/eor-1* ♂. These males were crossed with the *ekl-7* single mutants to generate progeny with the genotype *ekl-7/hT2; +/eor-1* ♀ with a Mendelian chance of 50%. At least 6 progeny from this cross were transferred to individual plates until the Uncoordinated (Unc) phenotype associated with *eor-1* was seen in subsequent non-green progeny.

To generate *ekl-7(vh20); lin-1(n2515) dpy-13(e184)* and *ekl-7(vh20); lin-1(n304)* double mutants, the same strategy as used above to generate *ekl-7; eor-1* mutants was used, except I looked for a dumpy (Dpy) phenotype linked to *lin-1(n2515)* and a Muv phenotype associated with *lin-1(n304)*.

To generate *ekl-7(vh20); eor-1(cs28); saIs14[plin-48::GFP)* transgenic double mutants, the *ekl-7; saIs14* strain was crossed with *+/hT2* ♂ to produce *ekl-7/ hT2; +/saIs14* ♂. These males were crossed into *ekl-7; eor-1* double mutants to generate hermaphrodite progeny with the genotype *ekl-7; +/eor-1; +/saIs14*. These animals were maintained until the Dpy phenotype segregated in animals expressing the *saIs14* transgene. The same strategy was used to bring in the *jcIs1* transgene.

To generate *ekl-7(vh20); lin-1(n2515) dpy-13(e184)* carrying either *saIs14[plin-48::GFP]* or *jcIs1[AJM-1::GFP; rol-6(su1006)]* transgenes, the same strategies as above were used.

To generate *ksr-1(n2526); csIs62[paff-1-NLS::GFP; grl-2::mRFP]* animals, *ksr-1* ♂ were generated and crossed into animals expressing the *csIs62* transgene. The resultant *ksr-1; +/ csIs62* ♂ crossed into *ksr-1* ☿ to ensure the *ksr-1* mutation was kept in the subsequent progeny. Animals were then maintained until the *csIs62* transgene expressed homozygously.

To generate *ekl-7(vh20); ksr-1(n2526); csIs62[paff-1-NLS::GFP; grl-2::mRFP]* transgenic double mutants, *+/hT2* ♂ were crossed into *ksr-1; csIs62* to produce male progeny with the genotype *+/hT2; ksr-1; csIs62/+*. These males were crossed with *ekl-7; ksr-1* ☿ to generate *ekl-7/ hT2; ksr-1; +/csIs62* ☿ with a Mendelian chance of 50%. At least 6 progeny from this cross were plated individually and screened for rod-like lethality and expression of the *csIs62* transgene.

Scoring rod-like lethality

Hermaphrodites for each genotype studied in this paper were grown on standard NGM plates at 20°C until they reached the L4 larval stage. Individual animals were then transferred to separate plates to develop into young adults and lay eggs for approximately 24 hours. Mothers were sacrificed and the number of eggs present on each plate was counted. After 24-48 hours, the number of remaining eggs and rod-like lethals were counted. The penetrance of rod-like lethality was calculated as follows: # of rods / (# of initial eggs - # of unhatched eggs). Only rods that were the approximate size of early L1-L2 larvae were included in the calculation as occasionally older larva died with rod-like characteristics.

Scoring of vulval cell specification

Animals at the early L4 larval stage were mounted on to glass microscope slides with a 2% agar pad, paralyzed with 100mM levamisole and visualized using an Axio Zeiss A1 Imager compound microscope with AxioVision software. Vulval induction was determined by Differential Interference Contract (DIC) microscopy. A vulval induction score for each animal was calculated by analyzing the descendants of each of the six VPCs, P3.p to P6.p and assigning them to either a vulval or non-vulval cell fates. If both the anterior and posterior daughters of a VPCs were induced, then this VPC would be given a score of 1. If only either the anterior or posterior daughter of a VPC was induced, then this VPC would be given a score of 0.5. A score of 0 was given to a VPC if both its daughters failed to divide. Therefore, a wild-type vulva would achieve a score of 3.0, an over-induced vulva (Muv) would achieve a score >3.0 with a maximum score of 6.0, and an under-induced vulva (Vul) would achieve a score <3.0 with a minimum score of 0. The average vulval induction score was calculated by adding the total number of VPCs induced and dividing the sum by the total number of animals observed.

Characterizing excretory ducts

The excretory ducts of hermaphrodite animals at the L1 larval stage were visualized using the A1 compound microscope. Two transgenes were used to deduce the identity and relative connectivity of the cells comprising the excretory system: *saIs14* which encodes for a transcriptional reporter of a duct-cell specific gene, *lin-48*, and *jcIs1* which encodes for a GFP-tagged marker for apical epithelial junction molecule, *AJM-1*. L1 larvae were mounted on glass microscope slides with a 2% agar pad and paralyzed with 5µL of 100mM levamisole.

Observing *aff-1* expression in early embryos

aff-1 expression was observed in early embryos by generating transgenic animals that expressed *csIs62,* a transgene that harbours a nuclear-localized transcriptional reporter for *aff-1* and *grl-2::mRFP*, a reporter that marks both the EDC and pore cell cytoplasm. Embryos recently laid by young adults were mounted on to glass microscope slides with a 2% agar pad and spread evenly with a piece of hair. Embryos were observed using the A1 compound microscope.

Construction of a rescue construct for *Y39G10AR.7,* pCR2.1_pekl-7_ekl-7_UTR-ekl-7

To generate a rescue construct for *Y39G10AR.7*, a 2.57kb DNA fragment that included the promoter, coding region, and 3' UTR of *Y39G10AR.7* was PCR amplified with the oligonucleotides JHo168_ekl-7 (5' - GTG TGC TTG GTG TTT TTT CG - 3') and JHo169_ekl-7 (5' - CTT TTT ATC ATT GGA TCT CAT AAT ACC C - 3') using High Fidelity (HF) Taq polymerase and DNA from wild-type lysates. This PCR fragment was then inserted into a pCR2.1 vector using T4 DNA ligase and the resulting 6.50kb plasmid was transformed by heat shock into DH5α competent cells, a bacterial strain of *E. coli* that is widely used for routine cloning procedures in the laboratory. Use of HF Taq polymerase avoided the need for the generation of sticky ends using restriction enzymes before ligation because HF Taq polymerase generates single-base adenine nucleotide overhangs that are complementary to single-base thymine nucleotide overhangs in the pCR2.1 vector. Successful transformants were screened for Ampicillin resistance and verified by DNA sequencing using sequencing primers M13_F, M13_R, PCo1, PCo2, PCo3, PCo4, PCo5, and PCo6 (sequences available in Table 5).

Construction of an N-terminal GFP fusion construct for *Y39G10AR.7*, pekl-7_GFP_ekl-7_6xHIS_UTR-unc-54

To generate an N-terminal GFP fusion construct for *Y39G10AR.7*, a 378bp DNA fragment covering the promoter of *Y39G10AR.7* was PCR amplified using the oligonucleotides PCo19_SphI_ekl-7 (5'- GAT ATT GCA TGC GTG TGC TTG GTG TTT TTT CG - 3') and PCo20_KpnI_ekl-7 (5' - GTC CTT GGT ACC CGC TGA AAT TTA TCA TTT AGA GTG - 3'). Another 1.67kb DNA fragment coding for the coding region of *Y39G10AR.7*, a 6xHIS tag and stop codon was PCR amplified using the oligonucleotides PCo21_BamHI_ekl-7 (5' - GAT ATA GGA TCC CCG GCC CCG AAA TTC ATC - 3') and PCo22_EcoRI_ekl-7 (5' - GTA TTA GAA TTC TTA GTG ATG ATG ATG ATG ATG ATC GTC ATC TTC CTC GTC TAT TTC ATC - 3'). A previously made backbone plasmid containing the desired GFP sequence, pvha-6_GFP_tbc-2-CC_UTR-unc-54, was digested with SphI and KpnI to remove pvha-6. After being digested with the same enzymes, the 378bp DNA fragment was ligated into the plasmid using T4 DNA ligase. The resulting plasmid, pekl-7_GFP_tbc-2-CC_UTR-unc-54, was then digested with BamHI and EcoRI to remove the tbc-2_CC domain. The 1.67kb DNA fragment was digested with the same enzymes and then ligated into the plasmid using T4 DNA ligase, resulting in the final construct, pekl-7_GFP_ekl-7_6xHIS_UTR-unc-54. The GFP fusion construct was transformed by heatshock into DH5α competent cells. Successful transformants were screened for Ampicillin resistance and verified by DNA sequence using sequencing primers PCo1, PCo3, PCo4, PCo5, PCo23, PCo24, PCo25, PCo26, JHo106, and JHo107 (sequences available in Table 5).

Microinjection and generation of extrachromosomal arrays

Microinjection is widely used technique in *C. elegans* to introduce and express DNA into animals that involves injection of an expression construct directly into the distal germline of a young adult hermaphrodite. Since the germ cell nuclei located in the distal gonad have a shared cytoplasm, injection of a DNA construct here occasionally produces large extrachomosomal arrays that express desired transgenes in the progeny of the injected mother [85][86]. To distinguish between animals that have taken up the transgene versus those that have not, the injection mixture often includes a co-injection construct that will be expressed alongside the desired transgene to allow screening for transgenic animals. In this study, my injection mixture consists of 20ng/μL of my DNA construct and 80ng/μL of *ttx-3::GFP*, my chosen co-injection marker. *ttx-3* has a role specifically in differentiation and axon outgrowth of an AIY interneuron pair located near the terminal bulb of the pharynx and is therefore easily identifiable by ultraviolet (UV) dissecting scope.

RNAi feeding protocol

RNAi feeding was performed as described previously [87]. Hermaphrodites were synchronized at the L1 stage using a standard bleaching protocol and allowed to grow on standard NGM plates until the L4 larval stage. Several L4 larva were then transferred on to RNAi plates seeded with a bacterial strain of *E. coli*, HT115, that express a desired RNAi clone. This particular strain encodes for T7 polymerase that is IPTG-inducible and is deficient of RNase III that would normally interfere with the production of dsRNA necessary to trigger RNAi. After approximately 24 hours of feeding, adults were either transferred to duplicate RNAi plates to

allow another cycle of egg laying or sacrificed if the number of embryos was already sufficient for scoring.

Construction of an RNAi clone for *Y39G10AR.7*

An RNAi clone for *Y39G10AR_246.h* was initially obtained from the Richard Roy lab at McGill University, Montréal, Québec, purchased as part of the Ahringer library, because this clone expressed a dsRNA that covered a locus that included *Y39G10AR.7*. Unfortunately, DNA sequencing revealed that this RNAi clone also covered a region upstream of *Y39G10AR.7* that included the neighbouring gene, *Y39G10AR.8*. Furthermore, rod-like lethality did not occur in *ksr-1* animals when they were fed with *Y39G10AR_246.h* RNAi.

I therefore generated a new RNAi clone by amplifying a 530 bp DNA fragment that covered the same region of *Y39G10AR.7* that included the predicted missense mutation for *vh20* using the oligonucleotides JHo156_BglII_ekl-7_RNAi (5' - CAA CAA GAT CTC TCC ATT GAC AGT CAC AAT G - 3') and JHo157_XhoI_ekl-7_RNAi (5' - CTG TAC TCG AGC TAA TCG TCA TCT TCC TCG TC - 3'). The DNA fragment was then cloned into a L4440 double-T7 vector using T4 DNA ligase and transformed into bacterial feeding strain HT115. Successful transformants were verified by DNA sequencing using sequencing primers L4440_F and L4440_R (sequences available in Table 5).

Test for efficacy of exogenous RNAi in *ruIs32* transgenic animals

To test for exogenous RNAi, I designed a simple test that would assay the efficacy of GFP RNAi in suppressing GFP expression in the germ cell nuclei of animals expressing a transgene, *ruIs32[ppie-1::GFP:H2B:pie-1; punc-119::unc-119(+)]*, that encodes a germline-specific GFP-tagged histone protein. By feeding these animals at the L4 stage RNAi for a gene predicted to be involved with small RNA biogenesis for 24 hours, then transferring young adults to new RNAi plates seeded with an equal mixture of RNAi for the gene of interest and GFP, the level of GFP expression in the germline of these animals could then be viewed using the Axio Zeiss A1 Imager compound microscope to determine if exogenous RNAi was functional (Figure 18A).

Results

ekl-7(vh20); ksr-1(n2526) animals have normal expression of *lin-48* in the EDC

The rod-like lethality observed in *ekl-7(vh20); ksr-1(n2526)* mutants suggested that these animals were failing to specify an EDC, a common trait seen in mutants that have reduced Ras signalling. In order to test this, I generated transgenic *ekl-7; ksr-1* double mutants expressing *saIs14*, a transgene that encodes a GFP under control of a duct-cell specific promoter, *lin-48*.

In *ksr-1(n2526)* animals that are essentially wild-type, I expectedly saw expression of *lin-48::GFP* in only a single cell in all animals observed (*n*=60), consistent with specification of the EDC. Unexpectedly, all *ekl-7(vh20); ksr-1(n2526)* animals (*n*=57) expressed the *lin-48::GFP* reporter in the EDC and one animal expressed *lin-48::GFP* in the EDC and pore cell (Figure 9). Despite this, several animals displayed extensive vacuolarization around the location of the excretory duct, an early sign of eventual rod-like lethality. This indicated that the excretory system in these animals had defects beyond specification of the EDC by criterion of *lin-48* expression.

ekl-7(vh20); ksr-1(n2526) animals have a defect in EDC autofusion

To determine whether any cell fate transformations may have occurred, I generated transgenic *ekl-7(vh20); ksr-1(n2526)* double mutants expressing *jcIs1*, a transgene that encodes a marker for apical epithelial junctions, *AJM-1*. In all *ksr-1* mutants (*n*=52), I observed the expected wild-type expression pattern of the *AJM-1* reporter: a triangular-like expression pattern corresponding

to the canal-EDC epithelial junction, a lack of expression where the EDC is presumed to be located, expression at the G1 pore autocellular junction, and expression where the G1 pore meets the epidermis. In 16 of 49 *ekl-7; ksr-1* mutants observed, the EDC maintained its autocellular junction (Figure 10), which would be consistent with a phenotype seen in mutants with reduced Ras signalling [60]. This suggests that *ekl-7* functions as a positive regulator of EDC fate with respect to EDC autofusion.

ekl-7(vh20); ksr-1(n2526) animals fail to express *aff-1* in the EDC

Autofusion of the EDC into a seamless toroid is known to be dependent on expression of a cell surface protein, AFF-1, which also regulates epithelial fusion of the anchor cell and lateral seam cells [62]. Since I observed a failure for the EDC to autofuse in *ekl-7(vh20); ksr-1(n2526)* mutants, a possibility was that the underlying cause for this was a failure to express *aff-1* at the particular time it was needed during development of the excretory duct.

To observe *aff-1* expression during embryogenesis, I generated *ksr-1(n2526)* and *ekl-7(vh20); ksr-1(n2526)* mutants carrying *csIs62*, a transgene that harbours both a green nuclear transcriptional reporter for *aff-1* (*paff-1-NLS::GFP*) and red marker for the EDC and pore cell cytoplasm (*grl-2::mRFP*). Importantly, these particular reporters express as early as the 1.5-fold stage during embryogenesis, allowing me to visualize *aff-1* expression in the EDC approximately when it autofuses to form a toroid. In *ksr-1* mutants, I observed *aff-1* expression in the nuclei of a cell that also expressed the *grl-2* reporter around the 2-fold stage embryo (Figure 11). Since the EDC and pore cell were too close to each other to distinguish at this stage, I also followed

embryos until the 3-fold stage when the cells began to take on more elongated shapes. Here, I observed *aff-1* expression specifically in the nucleus of a cell, which I identified as the EDC by its dorsal position to the other *grl-2*-expressing cell, which I presumed to be the G1 pore cell (Figure 12). In *ekl-7; ksr-1* mutants, 6/20 2-fold and 3-fold staged embryos failed to express *aff-1* in the nucleus of any *grl-2* positive cells, which would be consistent with previous data showing that these animals frequently have EDCs that fail to autofuse (Figure 12). Overall, these data suggest that *ekl-7* has a role in positively regulating *aff-1* expression specifically in the EDC during its specification.

ekl-7(vh20) animals have wild-type excretory ducts

To ensure the excretory defects seen in *ekl-7(vh20); ksr-1(n2526)* were not due to *ekl-7(vh20)* alone, I outcrossed *ksr-1* to generate *ekl-7(vh20)* single mutants and then brought in the same *lin-48::GFP* and *AJM-1::GFP* transgenes to characterize their excretory systems. I observed in all *ekl-7(vh20)* carrying the *lin-48::GFP* (*n*=36) and *AJM-1::GFP* (*n*=44) reporter that they had properly developed excretory ducts, where *lin-48::GFP* was expressed in a single EDC and *AJM-1::GFP* was expressed only at the epithelial junctions between the canal cell and EDC, and G1 pore autocellular junction (Figure 13). Consistent with this, *ekl-7(vh20)* animals are phenotypically wild-type and display no rod-like lethality (Table 1).

ekl-7(vh20); ksr-1(n2526) have essentially wild-type vulval cell specification

Since many downstream regulators have functions in multiple tissues, I wanted to determine whether *ekl-7* had a role in vulval development. An average vulval induction score was calculated as described in Materials and Methods. In *ekl-7(vh20); ksr-1(n2526)* animals, I calculated a vulval induction score of 2.98 (n=28) which was not significantly different from that expected for a wild-type vulva (Table 2). These mutants also fail to show any defects that would indicate vulval morphogenesis has been affected. This would suggest that *ekl-7* does not have a role during vulval development.

ekl-7(vh20) appears to function in parallel to *lin-1* and *eor-1*

Several reports demonstrate that downstream ERK substrates function synergistically during development of various tissues in *C. elegans*. LIN-1 and LIN-31, for example, form a heterodimer that directly binds DNA to regulate transcription of genes related to vulval induction [68]. LIN-1 and EOR-1 have also demonstrated cooperative function, whereby *lin-1* is converted from a transcriptional repressor to a transcriptional activator of vulval cell and EDC fates when *eor-1* is absent by a currently unknown mechanism [78][60]. Since EKL-7 has putative ERK phosphorylation and docking sites similar to those found on other ERK substrates, and my previous data indicate that *ekl-7* has a role specifically in the EDC, I hypothesized that EKL-7 may exhibit the same cooperativity with either LIN-1 or EOR-1 during EDC fate specification.

To test this, I crossed *ekl-7(vh20)* into either a *lin-1(n304)* or *eor-1(cs28)* loss-of-function genetic background and scored rod-like lethality in the double mutants. As with *lin-1(n304)* mutants, *ekl-7(vh20); lin-1(n304)* double mutants displayed no penetrance of rod-like lethality. Therefore, I decided to examine the effects of crossing in *ekl-7* with a known partial gain-of-function allele for *lin-1*, *n2515*, that alone showed a low penetrance of rod-like lethality. In both the *eor-1(cs28)* and *lin-1(n2515) dpy-13(e138)* mutant backgrounds, bringing in the *ekl-7(vh20)* mutation enhanced the penetrance of rod-like lethality seen in either of the *lin-1(n2515)* or *eor-1(cs28)* single mutants − 1.5% in *lin-1(n2515) dpy-13(e138)* to 18.4% *ekl-7(vh20); lin-1(n2515) dpy-13(e138)* and 16.0% in *eor-1(cs28)* to 33.8% in *ekl-7(vh20); eor-1(cs28)* (Figure 14). This result suggests that *ekl-7* functions in parallel to *lin-1* and *eor-1*.

ekl-7(vh20); eor-1(cs28) **animals sometimes specify 2 EDCs**

In order to understand why bringing *ekl-7(vh20)* into *eor-1(cs28)* might be enhancing rod-like lethality, I generated double mutants carrying the same transgenes used earlier to characterize the excretory duct, *saIs14* and *jcIs1*. In 4/32 *ekl-7; eor-1; saIs14* animals observed, I saw ectopic expression of *lin-48* in the G1 pore cell. Furthermore, I saw a similar frequency of *ekl-7; eor-1; jcIs1* animals that lacked a pore autocellular junction which would be consistent with a pore-to-EDC transformation (Figure 15). These data would suggest that *ekl-7* now behaves as a negative regulator of EDC fate when in the *eor-1(lf)* background. Interestingly, in many animals that correctly expressed the *lin-48* reporter in a single EDC, I noticed cyst-like formations in the EDC around the area where the duct is expected to narrow and join with the G1 pore (Figure 16).

Extensive vacuolarization in corresponding DIC images indicate that these cyst-like formations may be associated with rod-like lethality in these animals

ekl-7(vh20); lin-1(n2515) dpy-13(e138) animals appear to have a defect in the G1 pore autocellular junction

The same transgenes were used to characterize the excretory ducts in *ekl-7(vh20); lin-1(n2515) dpy-13(e138)* mutants. In all animals carrying the *saIs14* transgene (*n*=24), I saw expression of *lin-48::GFP* in a single EDC. Consistent with this observation, all animals carrying the *AJM-1::GFP* transgene showed no expression in the presumed location of the EDC, indicating that the EDC had properly autofused. Altogether, this suggests that the EDC fate was not affected by either *ekl-7(vh20)* or *lin-1(n2515) dpy-13*. Instead, I observed defects in the G1 pore autocellular junction, which showed a punctate-like expression pattern of *AJM-1::GFP*, where normally it should delineate a continuous epithelial junction (Figure 17). I do not know whether this phenotype underlies the enhancement in rod-like lethality observed in *ekl-7(vh20); lin-1(n2515) dpy-13(e183)* animals, but this result would suggest that *ekl-7* potentially has a role in regulating the pore autocellular junction.

The *vh20* allele may be a hypomorphic allele of *Y39G10AR.7*

The *vh20* mutation is predicted to be a missense mutation causing a change from a Lysine to Glutamic Acid residue (E422K) within a string of negatively charged amino acids at the C-terminal end of *Y39G10AR.7*. To begin characterizing the *vh20* allele, I generated an RNAi clone that targeted a 530 bp sequence on *Y39G10AR.7* and suppressed the gene in both

ksr-1(n2526) and *ekl-7(vh20); ksr-1(n2526)* animals. If *vh20* is a hypermorphic allele and rod-like lethality was related to overexpression of EKL-7, I would expect RNAi to suppress the phenotype. On the other hand, if *vh20* is a hypomorphic allele, RNAi would be expected to enhance rod-like lethality. Lastly, if *vh20* is a null allele, I would expect RNAi to have basically no effect on rod-like lethality.

I observed a rod-like lethality of 22.3% in *ksr-1(n2526); Y39G10AR.7(RNAi)* animals indicating that my clone was functional and that I had successfully targeted a gene involved with excretory duct development. I then performed the same RNAi test with *ekl-7(vh20); ksr-1(n2526); Y39G10AR.7(RNAi)* animals and saw an appreciable increase in rod-like lethality (41.3%) relative to the same animals fed with empty vector RNAi (Table 3). Assuming that *vh20* is indeed an allele of *Y39G10AR.7,* these results would suggest that RNAi is further suppressing *ekl-7* function in *ekl-7(vh20); ksr-1(n2526)* animals, and that the *vh20* is a hypomorphic allele.

Mosaically expressing a rescue construct for Y39G10AR.7 does not rescue rod-like lethality in *ekl-7(vh20); ksr-1(n2526)* mutants

To truly demonstrate that *vh20* is an allele of *Y39G10AR.7*, I attempted transgenic rescue of rod-like lethality using microinjection of a wild-type copy of *ekl-7*. I first generated an expression construct comprising the entire promoter, coding sequence, and 3' UTR of *Y39G10AR.7* using routine cloning procedures (see Materials and Methods) and microinjected the construct into the distal gonad of *ksr-1(n2526)* animals to generate *ksr-1(n2526); vhEx(Y39G10AR.7)* animals. I then crossed in *ekl-7* to generate *ekl-7(vh20); ksr-1(n2526); vhEx(Y39G10AR.7)* animals that

mosaically expressed a wild-type copy of *Y39G10AR.7* and scored rod-like lethality of both transgenic strains. Unfortunately, I did not see a significant difference in penetrance of rod-like lethality between *ekl-7(vh20); ksr-1(n2526)* transgenic versus non-transgenic animals, indicating that my construct had failed to rescue (Table 4). As well, I did not observe any rod-like lethality in *ksr-1(n2526); vhEx(Y39G10AR.7)* beyond what would be expected for *ksr-1(2526)* animals indicating that exogenous expression did not cause a rod-like lethal phenotype.

Suppression of *Y39G10AR.7* does not appear to affect exogenous RNAi

Y39G10AR.7 was identified in a genome-wide screen for genes involved with transgene silencing and endogenous RNAi silencing [88]. Defective endogenous RNAi silencing was sensed by silencing activity of an endogenous siRNA, siR-1, in a sensor strain that contained a transgene encoding an insert that was the reverse complement of siR-1 [88][89]. In wild-type animals, siR-1 normally targets a non-coding RNA, *linc-22*, but in the sensor strain due to co-suppression, the transgene will also be inactivated allowing endogenous RNAi function to be probed. Inactivation of *Y39G10AR.7* was reported to enhance transgene silencing of 3 of 5 integrated multicopy transgenes used in the screen, and also cause defective endogenous RNAi indicated by a desilencing of siR-1. Transgene silencing and small RNAi pathways are known to share many of the same core components and accordingly, animals with enhanced transgene silencing show a similar enhancement in exogenous RNAi [90]. Interestingly, many of the *ekl* genes that were identified in the genome-wide RNAi screen that also pulled out *Y39G10AR.7* were putative regulators of small RNA pathways, including germline Argonaute *csr-1*, Dicer-related helicase *drh-3*, RNA-directed RNA polymerase *ego-1*, and Tudor-domain *ekl-1* [44].

Therefore, I wanted to test if inactivation of *Y39G10AR.7* also caused an associated effect on exogenous RNAi. I conducted a simple assay to test whether *Y39G10AR.7* had a potential role in the exogenous RNAi pathway involving simultaneous RNAi suppression of *Y39G10AR.7* and GFP in a strain that expressed a transgene, *ruIs32*, encoding a germline-specific GFP-tagged histone, H2B (see Materials and Methods) (Figure 18A). In animals fed both GFP RNAi with *Y39G10AR.7* RNAi, I saw no GFP expression in the germline nuclei that would indicate that exogenous RNAi worked effectively. On the contrary, animals fed GFP RNAi with *csr-1* RNAi in my positive control showed moderate nuclear GFP expression, consistent with a requirement for *csr-1* in the exogenous RNAi pathway (Figure 18B). Therefore, my data is not consistent with *Y39G10AR.7* being required for exogenous RNAi.

Discussion

Cell signalling allows individual cells to communicate with one another, remain responsive to extracellular cues, and coordinate cellular events that are integral to proper animal development. In *C. elegans*, the evolutionarily conserved EGFR/Ras/MAPK signalling pathway is repeatedly used to regulate development of numerous tissues and organs [19]. While core components of this pathway and their effects on general signalling are well characterized, it remains unclear how Ras signalling is regulated downstream. The ability for a single signalling pathway to regulate so many biological processes likely relies on the suite of downstream ERK targets and their ability to shape signalling outputs in a tissue-specific manner. The goal of this study was to begin characterizing *ekl-7(vh20)*, a mutation that is likely in a gene that codes for a novel putative ERK substrate and regulator of EDC fate specification.

ekl-7(vh20) was initially identified in an EMS mutagenesis screen for enhancers of *ksr-1* lethality and showed a penetrance of rod-like lethality of 31%, but no other overt phenotypes in the vulva or other tissues regulated by Ras signalling. Chromosome and interval mapping of *vh20* placed it to the left arm of chromosome I, and subsequent whole genome sequencing identified a strong candidate for the mutation, *Y39G10AR.7*. Protein sequence analysis of Y39G10AR.7 show the presence of several conserved ERK docking and ERK phosphorylation sites similar to those found on other ERK substrates LIN-1 and EOR-1, suggesting that Y39G10AR.7 may be a downstream target as well. Mutations in either *lin-1* or *eor-1* result in pleiotropic effects in several tissues, namely the excretory duct and vulva. Since *Y39G10AR.7* (which I have since renamed *ekl-7*) appeared to have functions specifically in the EDC, I wanted to investigate

further how it might regulate Ras/MAPK signalling and/or function with *lin-1* and *eor-1* during development of the excretory duct.

A common cause of rod-like lethality in Ras mutants is a failure to specify an EDC since Ras/MAPK signalling promotes the EDC fate over the G1 pore cell fate in one of the epithelial progenitors during excretory duct development [56][57][60]. However, I observed that all *ekl-7(vh20); ksr-1(n2526)* mutants expressed a duct-cell specific reporter for *lin-48* in a single cell, suggesting an EDC had been properly specified by that criterion. Instead, about a third of these animals have an EDC that failed to autofuse and maintained its autocellular junction like a pore cell, suggesting that the EDC fate was not specified properly and that *ekl-7* behaves as a positive regulator of EDC fate. These results are different from what has been previously reported; mutants with reduced Ras signalling typically fail to express *lin-48* in the EDC and have an EDC that fails to autofuse within the same animal, but here when *ekl-7* is mutated, only the EDC fails to autofuse [60]. Therefore, my results suggest that the EDC in *ekl-7(vh20); ksr-1(n2526)* mutants is only partially specified and that *ekl-7* has a specific role during autofusion of the EDC.

Autofusion of the EDC is known to be dependent on a cell surface fusogen, *aff-1*, that mediates numerous epithelial fusion events during *C. elegans* development. Since I observed a specific defect in EDC autofusion in *ekl-7(vh20); ksr-1(n2526)* mutants, a logical explanation was that *aff-1* expression was defective in these animals. To test the possibility, I generated *ekl-7(vh20); ksr-1(n2526)* double mutants carrying a transgene that harboured a nuclear transcriptional

reporter for *aff-1* expression and a marker for the EDC and G1 pore cell, and expresses at an early stage of embryogenesis. In 2-fold to 3-fold staged *ekl-7(vh20); ksr-1(n2526)* embryos, I observe that nearly a third of the embryos had EDCs that failed to express *aff-1* at the time when EDC autofusion was expected to occur. In *ksr-1(n2526)* animals carrying the same transgene, *aff-1* expression was always observed in the nucleus of the EDC. These results would be consistent with the failure to autofuse phenotype I observed in the EDCs. Altogether, my data suggest that *ekl-7* is a specific regulator of *aff-1* expression in the EDC. What remains to be understood is how autofusion of the EDC is related to the overall functionality of the excretory system in these animals. It has been reported that withdrawal of the G1 pore may be an intrinsic trait of the G1 pore and EDC progenitors that is inhibited by Ras/MAPK signalling, and that autofusion of the EDC around the pore cell may contribute to its permanence in the excretory system [60]. *aff-1* mutants also have EDCs that fail to autofuse but do not display any associated rod-like lethality [43]. Therefore, a failure to express *aff-1* does not fully explain the rod-like phenotype. Thus, additional defects must underlie the phenotypes seen in *ekl-7(vh20); ksr-1(n2526)* animals.

Synergistic function is a common theme between downstream ERK substrates and demonstrate the ability for many regulators of Ras signalling to control development in a tissue-specific manner. For example, LIN-1 and EOR-1 have been reported to have cryptic cooperative function during specification of EDC fate and induction of vulval cell fates [73][75]. Since I hypothesized that EKL-7 is putative ERK substrate, I thought it might share the same behaviour with either LIN-1 or EOR-1 during specification of the EDC. My data show that *ekl-7(vh20);*

lin-1(n2515) and *ekl-7(vh20); eor-1(cs28)* double mutants display an enhancement in rod-like lethality relative to that seen in either of the individual *lin-1* or *eor-1* mutant backgrounds, suggesting that *ekl-7* functions in parallel to *lin-1* and *eor-1* during excretory duct development.

In order to understand how the excretory duct might be being affected in *ekl-7(vh20); lin-1(n2515)* and *ekl-7(vh20); eor-1(cs28)* double mutants, I made use of the same two reporters used earlier to characterize and identify cells of the system. 4 of 32 *ekl-7(vh20); eor-1(cs28)* animals carrying the duct-cell specific *lin-48::GFP* reporter showed ectopic expression in a second cell, presumably a G1 pore cell now adopting a EDC-like fate. A similar percentage of animals carrying the *AJM-1::GFP* reporter had a G1 pore cell in which the autocellular junction fused, consistent with the idea of a pore-to-EDC transformation typical of *Ras(gf)* mutants. *ekl-7(vh20)* had a positive role in specification of the EDC in the *ksr-1(n2526)* background, but appears to have a negative role when in the *eor-1(cs28)* background. This apparent switch in role in terms of Ras signalling is similar to what was observed between *lin-1(n304)* and *eor-1(cs28)* mutants, where *lin-1* normally negatively regulates the EDC fate but demonstrates a strong positive requirement in the *eor-1* background [78]. Since neither *ekl-7(vh20)* mutants nor animals fed RNAi for *vh20* showed any obvious phenotypes, *ekl-7* probably does not have an essential role in the pathway, though a null allele of *ekl-7* would be needed to be certain of this. A possibility is that the different phenotypes I have observed for *ekl-7* when in either the *ksr-1* or *eor-1* backgrounds might be a reflection of the dual roles of *lin-1* during EDC specification. Interestingly, *ekl-7(vh20); eor-1(cs28)* mutants that properly specified a single EDC commonly had cyst-like formations near the ventral side of the EDC where it meets the G1 pore cell,

indicating that these mutants still had defects in the excretory duct beyond expression of two cell fate markers. A similar phenotype has been reported in mutants for *lpr-1*, a lipocalin required for connectivity of the EDC and G1 pore lumina [43]. This could suggest that the enhancement in rod-like lethality observed in these double mutants is related to a defect in luminal connectivity between the G1 pore and EDC, but further experimentation would be needed to substantiate this idea.

ekl-7(vh20); lin-1(n2515) double mutants show no defects in EDC specification by criteria of *lin-48::GFP* expression or EDC autofusion. Instead, I surprisingly observed defect in the G1 pore autocellular junction, where the *AJM-1::GFP* reporter expressed in a disconnected and interspersed fashion rather than in a continuous one seen in wild-type animals. I currently do not know how this unusual pore phenotype underlies the enhancement in rod-like lethality observed in *ekl-7(vh20); lin-1(2515)* mutants. A possibility is that the pore autocellular junction is only partially formed and meeting at scattered points and therefore cannot fully seal off the pore lumen, therefore promoting leakiness of the system.

I began to attempt to characterize the *vh20* allele by testing the effects of suppressing *Y39G10AR.7* in *ksr-1(n2526)* and *ekl-7(vh20); ksr-1(n2526)* animals through use of an RNAi clone I made. *ksr-1(n2526)* treated with *ekl-7(RNAi)* showed partial penetrance of rod-like lethality which would consistent with the idea that *Y39G10AR.7* is an *ekl*. *ekl-7(vh20); ksr-1(n2526)* animals treated with RNAi demonstrated a slight enhancement in rod-like lethality relative to those fed with empty vector RNAi, which suggests the *vh20* allele is hypomorphic.

Further biochemical data would be needed to truly determine the effects of *vh20* on expression of *ekl-7*, however.

To fully confirm *vh20* as an allele for *Y39G10AR.7*, I attempted to rescue the rod-like lethality seen in *ekl-7(vh20); ksr-1(n2526)* mutants by making them express a transgenic wild-type copy of *Y39G10AR.7*. Unfortunately, I failed to observe any rescue in transgenic animals generated by microinjection. This result could suggest a number of things: firstly, *vh20* may not be an allele of *Y39G10AR.7*. If this were the case, my data relating to the effects of *ekl-7(vh20)* on specification of the EDC in various mutants and those from my RNAi experiments should be treated separately. A large caveat of using microinjection to generate transgenic animals is that this method causes mosaic expression of the injected transgene as an extrachromosomal array. In other words, I would not know whether my rescue construct is expressing in the right cells or at the right time when it is needed. It is well known in *C. elegans* that foreign DNA and transgenes are potently silenced in the germline by endogenous RNAi as a way to maintain germline genome integrity. If *Y39G10AR.7* was required maternally in the germline, expression of my rescue construct would be silenced. Indeed, *Y39G10AR.7* clustered with several genes with germline expression profiles based on transcriptional co-regulation [88].

In summary, I have demonstrated that *ekl-7* functions as a positive regulator of partial EDC fate by regulating expression of *aff-1* specifically in the EDC during its requirements in early embryogenesis when the EDC autofuses into a seamless toroid (Figure 19). Interestingly, *aff-1* is not known to be an essential factor for excretory duct function, suggesting *ekl-7* likely has roles

in determining other aspects of EDC fate. Moreover, I have also supported the idea that EKL-7 is a putative ERK substrate by showing that EKL-7 functions synergistically with ERK substrates, LIN-1 and EOR-1, during excretory duct development. Little is known about how Ras/MAPK signalling is regulated at a tissue-specific level to control particular aspects of animal development. As a specific regulator of the EDC fate, EKL-7 may define an important specificity factor that promotes the EDC fate over other cell fates governed by Ras/MAPK signalling by working in conjunction with general downstream effectors LIN-1 and EOR-1.

Future Directions

In addition to what has already been mentioned, there are a number of experiments that should be done to further my understanding of *ekl-7* as a regulator of Ras/MAPK signalling. First and foremost, a different method should be used to rescue rod-like lethality in *ekl-7(vh20); ksr-1(n2526)* mutants that would avoid problems associated with mosaic expression and silencing of my rescue construct in the germline. By cloning *Y39G10AR.7* under a germline-specific promoter, *ppie-1*, and making appropriate adjustments to the 3' UTR if needed, my rescue construct would avoid being silenced. I could also use CRISPR/Cas9 technology to create a large deletion in *Y39G10AR.7* to generate a null allele for the gene and then cross that mutation into the *ekl-7(vh20); ksr-1(n2526)* background in a complementation test. Alternatively, CRISPR/Cas9 may be used to generate the same predicted point mutation for *vh20* in *Y39G10AR.7* in *ksr-1* animal to see if the resulting CRISPR mutants display a similar rod-like lethality seen in *ekl-7(vh20); ksr-1(n2526)*. Vice-versa, CRISPR/Cas9 could be used to simply correct the predicted *vh20* missense mutation in *ekl-7(vh20); ksr-1(n2526)* animals to see if this

rescues rod-like lethality. This method could also be used simultaneously to generate new alleles for *Y39G10AR.7* and identify important domains in its protein sequence. For example, it may identify which of the putative ERK docking and phosphorylation sites are important to its function. An advantage of CRISPR/Cas9 is that all gene modifications would be driven by their endogenous promoter and therefore avoids all previously mentioned problems with expression of transgenic extrachromosomal arrays.

Localization experiments to determine the subcellular localization of Y39G10AR.7 would provide great insight to its cellular function. If it is indeed nuclear, this could suggest a potential role as a transcription factor similar to other downstream MPK-1/ERK targets. If it is cytoplasmic, then this would suggest Y39G10AR.7 functions at another step in the Ras/MAPK pathway. I have generated an N-terminal GFP fusion construct (see Materials and Methods) which will be used to generate *ksr-1; vhEx(GFP::Y39G10AR.7::6xHIS)* transgenic animals. The array can also be subsequently crossed into *ekl-7(vh20); ksr-1(n2526)* animals to test for rescue using another construct that expresses wild-type *Y39G10AR.7.*

I have shown that *ekl-7(vh20); eor-1(cs28)* and *ekl-7(vh20); lin-1(n2515)* mutants have enhanced rod-like lethality relative to that seen in *eor-1(cs28)* and *lin-1(n2515)* single mutants, and that these double mutants have various defects in excretory duct development. However, it is still unclear as to how the functionality of the excretory system has been affected by these defects. In *ekl-7(vh20); eor-1(cs28)* mutants, cyst-like formations in the EDC indicate fluid is being backed up at a particular location in the duct, suggesting there may be a luminal defect

somewhere in the system. To test this, a fluorescent luminal marker could be used in conjunction with an EDC and G1 pore reporter (i.e. *grl-2::m*RFP) to identify potential defects in luminal connectivity between the EDC and G1 pore in these animals. Use of the luminal marker in *ekl-7(vh20); lin-1(n2515)* mutants may also help uncover if the G1 pore autocellular junction is of direct consequence to its function or a byproduct of an unseen luminal defect.

I observed that *ekl-7* has a specific role in the EDC when in the *ksr-1* mutant background and that *ekl-7(vh20); eor-1(cs28)* and *ekl-7(vh20); lin-1(n2515)* mutants have particular excretory duct defects, but *eor-1* and *lin-1* are known to have roles in multiple tissues. It will be necessary to study the vulva in these mutants to see if development has been affected there as well. The *ekl-7(vh20); lin-1(n304)* mutants that I generated, for example, were completely viable and showed no apparent defects in excretory duct development, but may have subtle changes in vulval induction that would implicate *ekl-7* in those tissues as well. Therefore, a good follow up would be to score vulval induction in each of these mutants to provide more insight as to how these effectors may be regulated during vulval development.

The presence of numerous ERK docking and phosphorylation sites on Y39G10AR.7 makes it a likely MPK-1/ERK substrate. To investigate this possibility, a good experiment to conduct would be an *in vitro* kinase assay using mammalian ERK2 and Y39G10AR.7. If found as an *in vitro* ERK2 substrate, it may be determined *in vivo* whether Y39G10AR.7 is phosphorylated by assessing its mobility by SDS/PAGE using worm lysates derived from wild-type and *mpk-1* mutants. A potential follow up to this experiment would be to perform site-directed mutagenesis

on residues within each putative ERK phosphorylation and docking site to identify their functional importance.

Taken altogether, these additional experiments would more fully characterize the role of *ekl-7* as either a specific or general regulator of Ras/MAPK signalling during early embryogenesis. Understanding how *ekl-7* functions may provide insight as to why loss of general downstream effectors like *lin-1* and *eor-1* often have pleiotropic effects and how this pathway is used repeatedly during animal development.

Figure 1

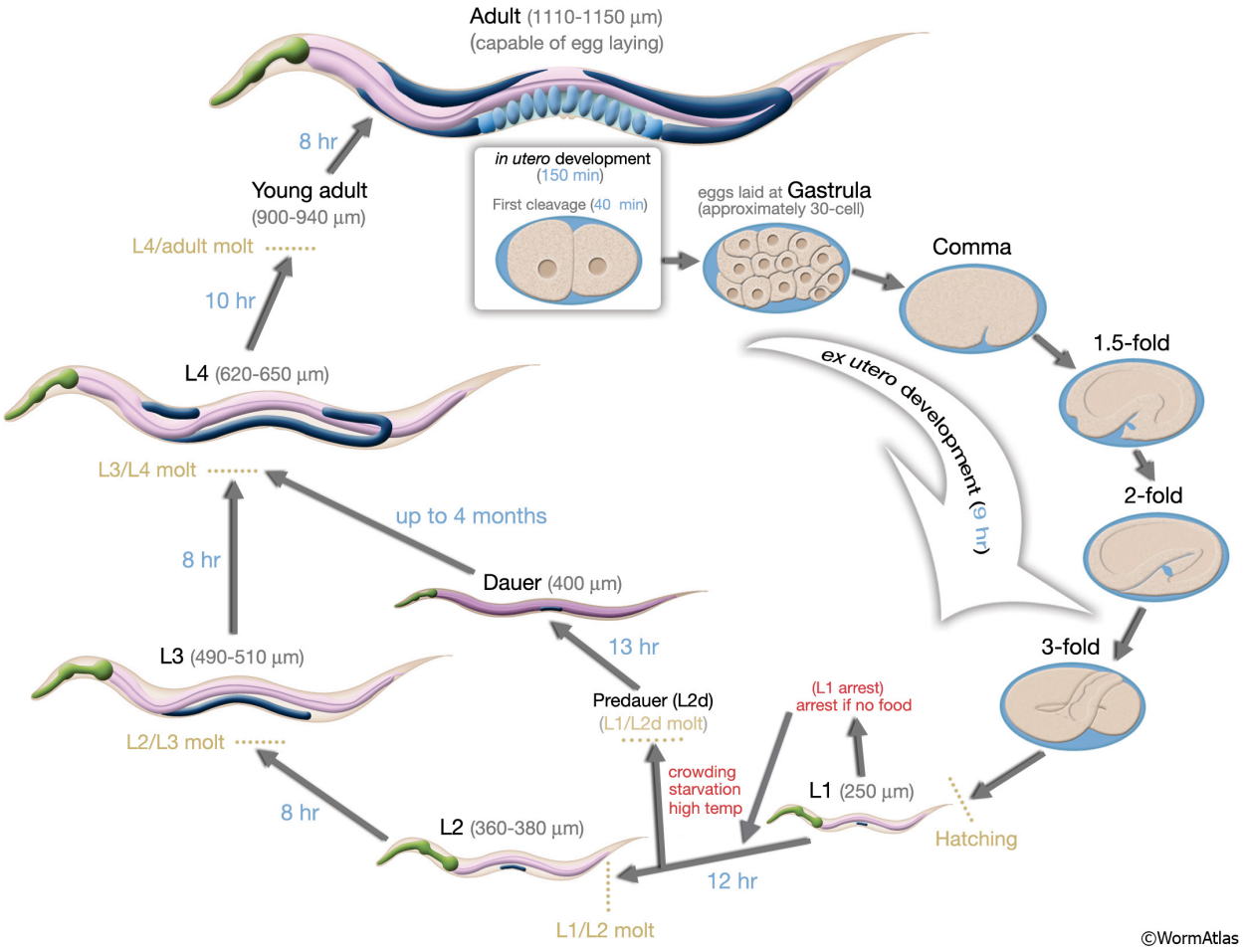

Figure 1: Life Cycle of *C. elegans*

The life cycle of a wild-type hermaphroditic *C. elegans* consists of an embryonic stage, four larval stages (L1-L4), and adulthood. Embryogenesis involves periods of cell proliferation and followed by extensive cell rearrangements leading to establishment of the animal's main body plan by hatching. The four larval stages are characterized by periods of inactivity where the animal will molt its old cuticle and form a new one in its place. L2 larvae may enter a dauer stage if environmental conditions are unfavourable for further development. Adults are capable of laying eggs for around 4 days.

Figure 2

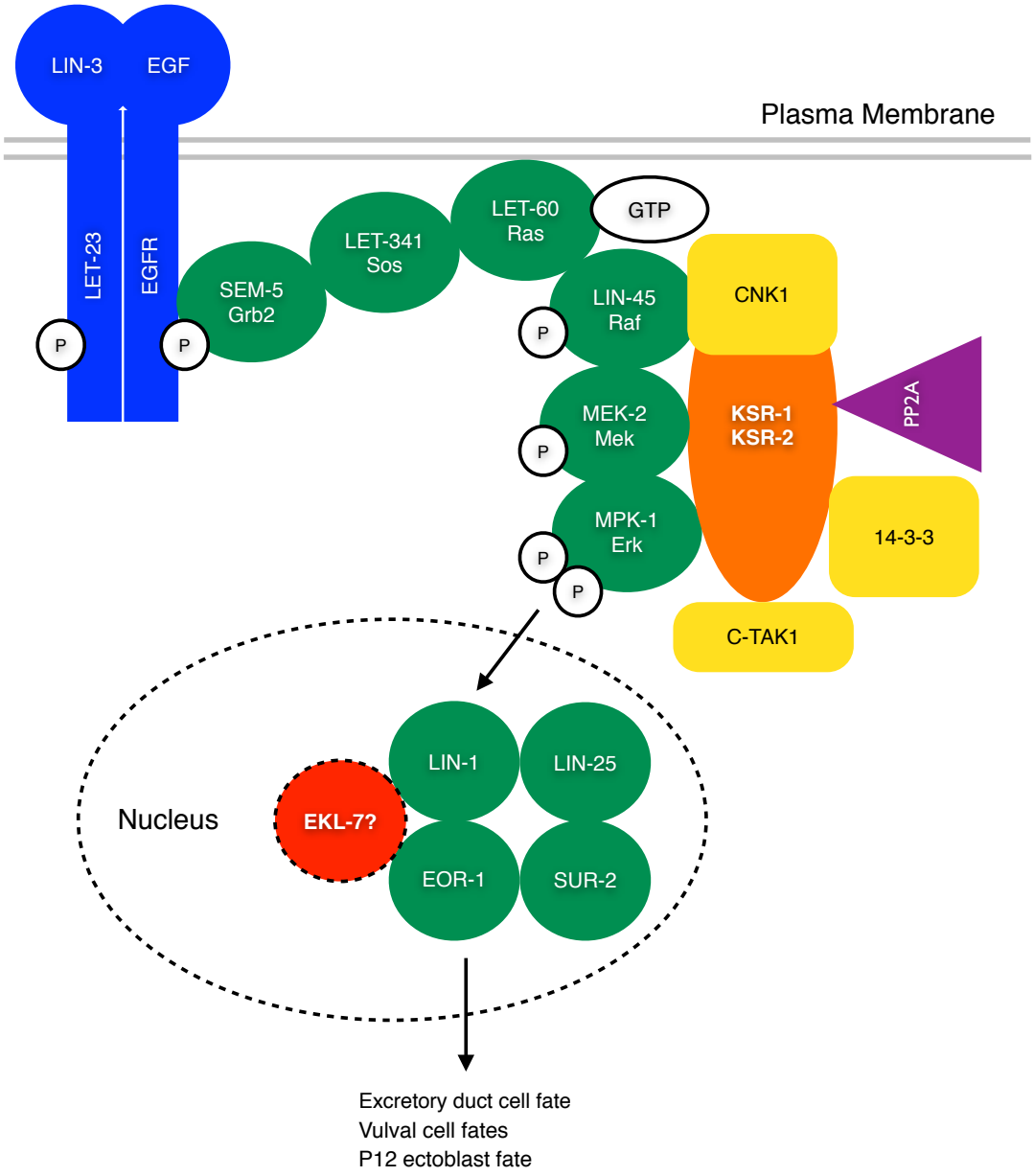

Figure 2: EGFR/Ras/ERK signalling pathway in *C. elegans*
LET-23/EGFR is activated by LIN-3/EGF which causes receptor dimerization and trans-autophosphorylation of tyrosine residues on their cytoplasmic tails. These phosphotyrosines act as binding sites for SEM-5/GRB-2 adaptor protein, which itself then recruits LET-341/SOS to the plasma membrane. LET-341/SOS is a GEF that activates LET-60/Ras, stimulating the MAPK cascade consisting of LIN-45/Raf, MEK-2/MEK, and MPK-1/ERK. The EGFR/Ras/ERK signalling pathway is used during determination of EDC, vulval cell, and P12 ectoblast cell fates.

Figure 3

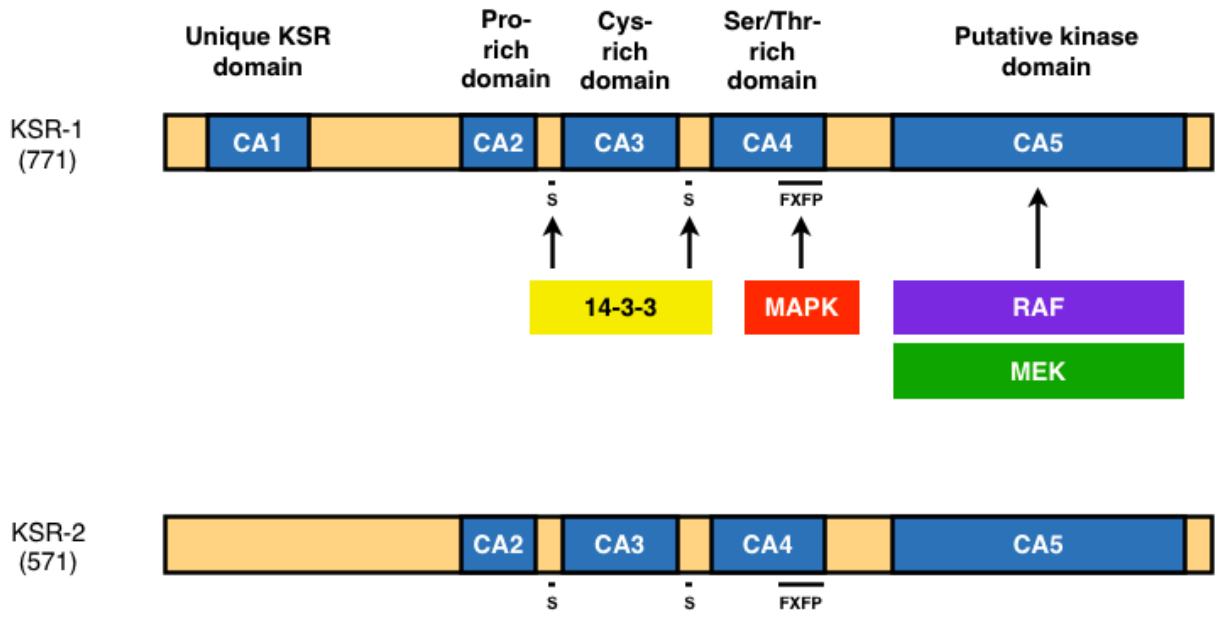

Adapted from Morrison *et al.*, 2001

Figure 3: KSR isoforms in *C. elegans*
Schematic of the structure of KSR isoforms, KSR-1 and KSR-2, along with associated conserved domains, motifs, and binding partners. KSR proteins have 5 conserved domains: CA1, a domain unique to KSR; CA2, a proline-rich domain; CA3, a cysteine-rich domain; CA4, a serine/ threonine-rich domain that contains a consensus MAPK binding motif FXFP; and CA5, a putative kinase domain. The CA1 domain is lacking in KSR-2. 14-3-3 binds phosphoserine residues located around the CA3 domain and is thought to stabilize KSR in an inactive form.

Figure 4

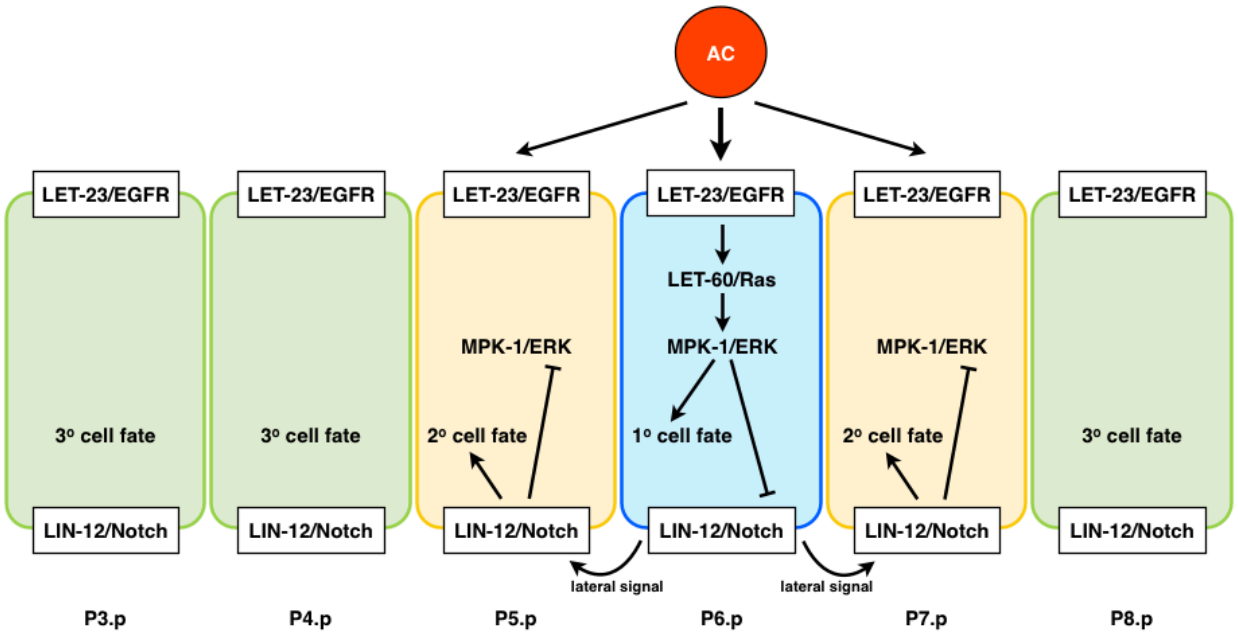

Adapted from Yoo *et al.*, 2004

Figure 4: Vulval patterning
A LIN-3/EGF gradient produced by the anchor cell (AC) stimulates LET-23/EGFR on VPCs P5.p, P6.p, and P7.p, but P6.p receives the strongest LIN-3 signal. Activation of downstream MPK-1/ERK in P6.p causes it to adopt a primary (1º) vulval cell fate. P6.p produces a lateral signal that stimulates LIN-12/Notch on P5.p and P7.p which inhibits MPK-1/ERK, thus preventing these cells from adopting a 1º vulval cell fate and instead adopting secondary (2º) vulval cell fates. The peripheral cells that do not receive a LIN-3/EGF inductive signal take on tertiary (3º) non-vulval cell fates and eventual fuse with the Hyp7 epidermis.

Figure 5

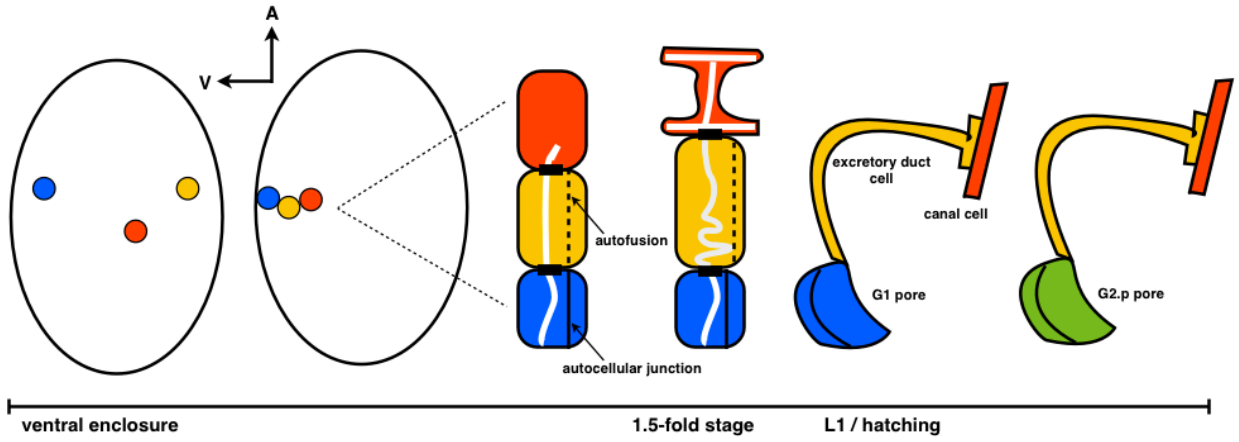

Adapted from Abdus-Saboor *et al.*, 2011

Figure 5: Stages of excretory duct development
Excretory duct development begins during ventral enclosure of embryogenesis, when the epithelial progenitors of the canal cell (red), EDC (yellow), G1 pore cell (blue). The canal cell produces a LIN-3/EGF inductive signal that promotes the EDC fate over the pore fate in the initially equivalent EDC and G1 pore progenitors. Around the 2-fold to 3-fold stage, both cells compete for the canal cell-proximal position, but due to left asymmetric biased position of the EDC progenitor, it reaches the canal cell first, adheres, and adopts the EDC fate. The G1 pore progenitor thus takes on the most ventral position and adopts a pore cell fate. After meeting, the EDC and G1 pore cell wrap around and form autocellular junctions, but only the EDC autofuses into a seamless toroid. The excretory duct now consists of three tandemly-linked unicellular tubes with a shared lumen. The system undergoes extensive morphogenesis and elongation before it is completely function upon hatching. Around the L2 stage, the G1 pore is replaced by the posterior daughter of a nearby G2 epidermal cell.

Figure 6

A

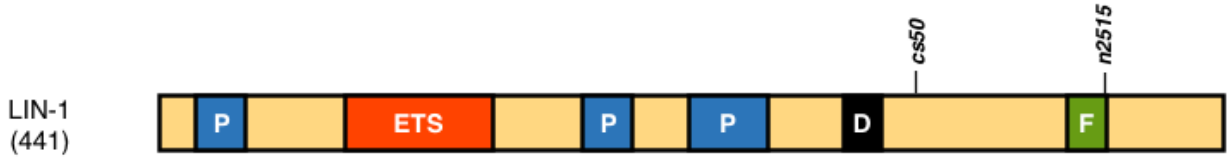

B

```
                                    ETS domain
hETS-1      ------------------------IQLWQFLLELLTDKSCQSFISWTG-DGWEFKLSDPDE 36
hETS-2      ------------------------IQLWQFLLELLSDKSCQSFISWTG-DGWEFKLADPDE 36
hELK-1      ---------------------MDPSVTLWQFLLQLLREQGNGHIISWTSRDGGEFKLVDAEE 41
ceLIN-1     MNVSDLMCTRSSTPPTSSSVDSIITLWQFLLELLQQDQNGDIIEWTRGTDGEFRLIDAEA 60
                                 : ******:** :.    :*.**   . **:* *.:
                          ETS domain
hETS-1      VARRWGKRKNKPKMNYEKLSRGLRYYYDKNIIHKTAGKRYVYRFV--------------- 81
hETS-2      VARRWGKRKNKPKMNYEKLSRGLRYYYDKNIIHKTSGKRYVYRFV--------------- 81
hELK-1      VARLWGLRKNKTNMNYDKLSRALRYYYDKNIIRKVSGQKFVYKFVSYPESHCAP------- 95
ceLIN-1     VARKWGQRKAKPHMNYDKLSRALRYYYEKNIIKKVIGKKFVYRFVT-TDAHAPPTADFSS 119
            *** ** ** *.:***:****.*****:****:*. *:::**:**
```

Figure 6: LIN-1, ETS-domain-containing transcription factor
[A] Schematic of LIN-1 protein showing the predicted PEST domains (P), ETS domain, D domain (D), and FXFP motif (F). Positions of relevant *lin-1* missense mutations are shown. *n2515* is located in the FXFP motif and prevents negative regulation by MPK-1/ERK. *n304* is located in the ETS domain and affects the ability for LIN-1 to bind DNA. *cs50* is located in one of the 18 putative MPK-1/ERK phosphorylation sites of LIN-1 that also is involved with its negative regulation. *n304* causes a deletion of exons 3 and 4, and rearrangement of exons 5 and 6 (not shown). [B] BLASTp alignment of *C. elegans* LIN-1 (CeLIN-1) with human ETS transcription factors ETS-1 (hETS-1), ETS-2 (hETS-2), and ELK-1 (hELK-1) reveals strong homology at the putative ETS domain (bracketed above). The ETS domain of CeLIN-1 shares 59% identity with both hETS-1 and hETS-2, and shares 67% identity with hELK-1.

Figure 7

A

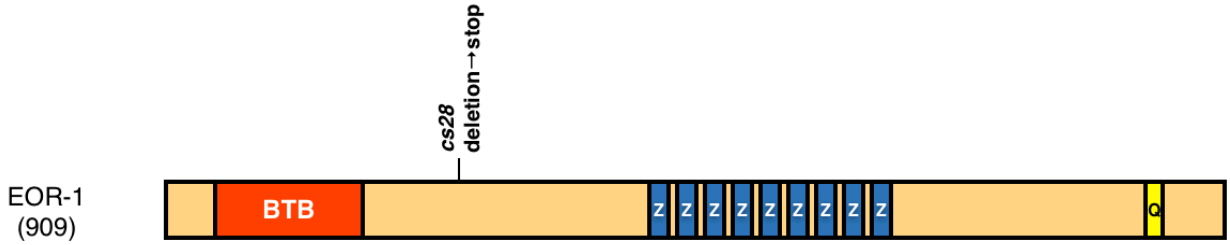

B

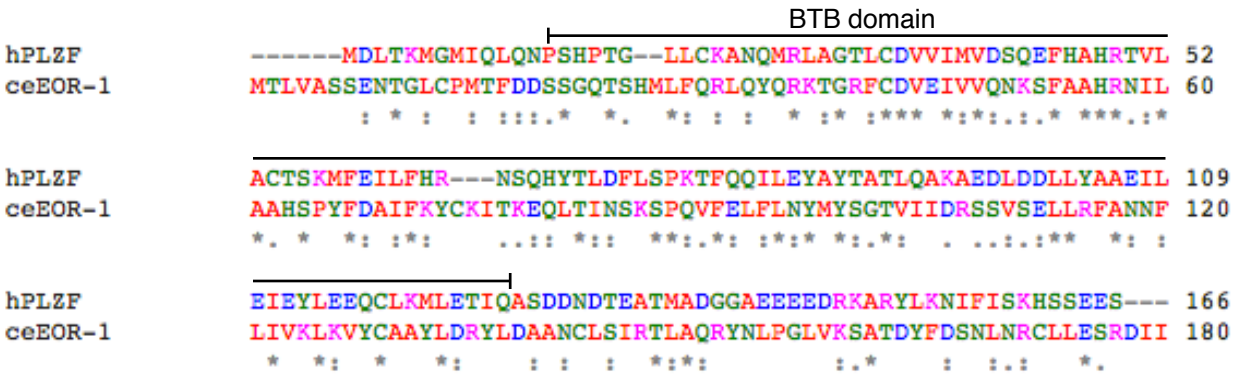

Figure 7: EOR-1/PLZF transcription factor
[A] Schematic of EOR-1 protein showing its N-terminal BTB domain and nine C2H2 zinc-finger domains (Z) that are capable of binding the major groove of DNA. *In vitro* studies demonstrate that regulation of EOR-1 is dependent on an MPK-1 ERK phosphorylation site located in its BTB domain. A polyglutamine tract is located near the C-terminal end of the protein (Q) The location of the *cs28* deletion that results in a premature stop is shown. [B] BLASTp alignment of *C. elegans* (ceEOR-1) with human PLZF (hPLZF) shows strong homology over the BTB domain and C2H2 zing finger domains (not shown). The BTB domain of ceEOR-1 shares 31% identity with that of hPLZF.

Figure 8

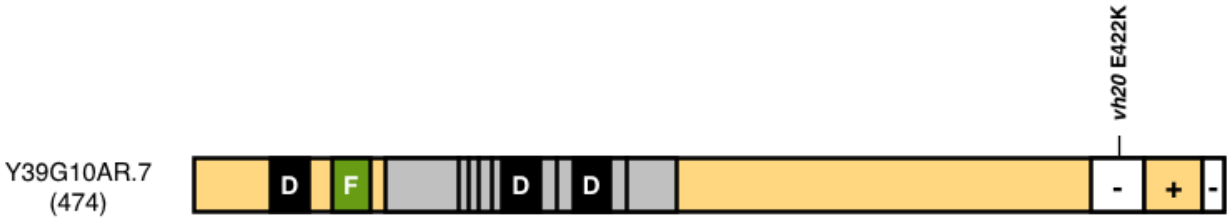

Figure 8: Y39G10AR.7/EKL-7
Schematic of Y39G10AR.7 protein showing the putative MPK-1/ERK phosphorylation sites (P-S/T-XP or S/T-P shown as vertical lines in grey) and docking sites (FXFP or D domain), and the location of the E422K missense mutation predicted to be *vh20*. C-terminal spans of negative (-) and positive (+) residues are also indicated.

Figure 9

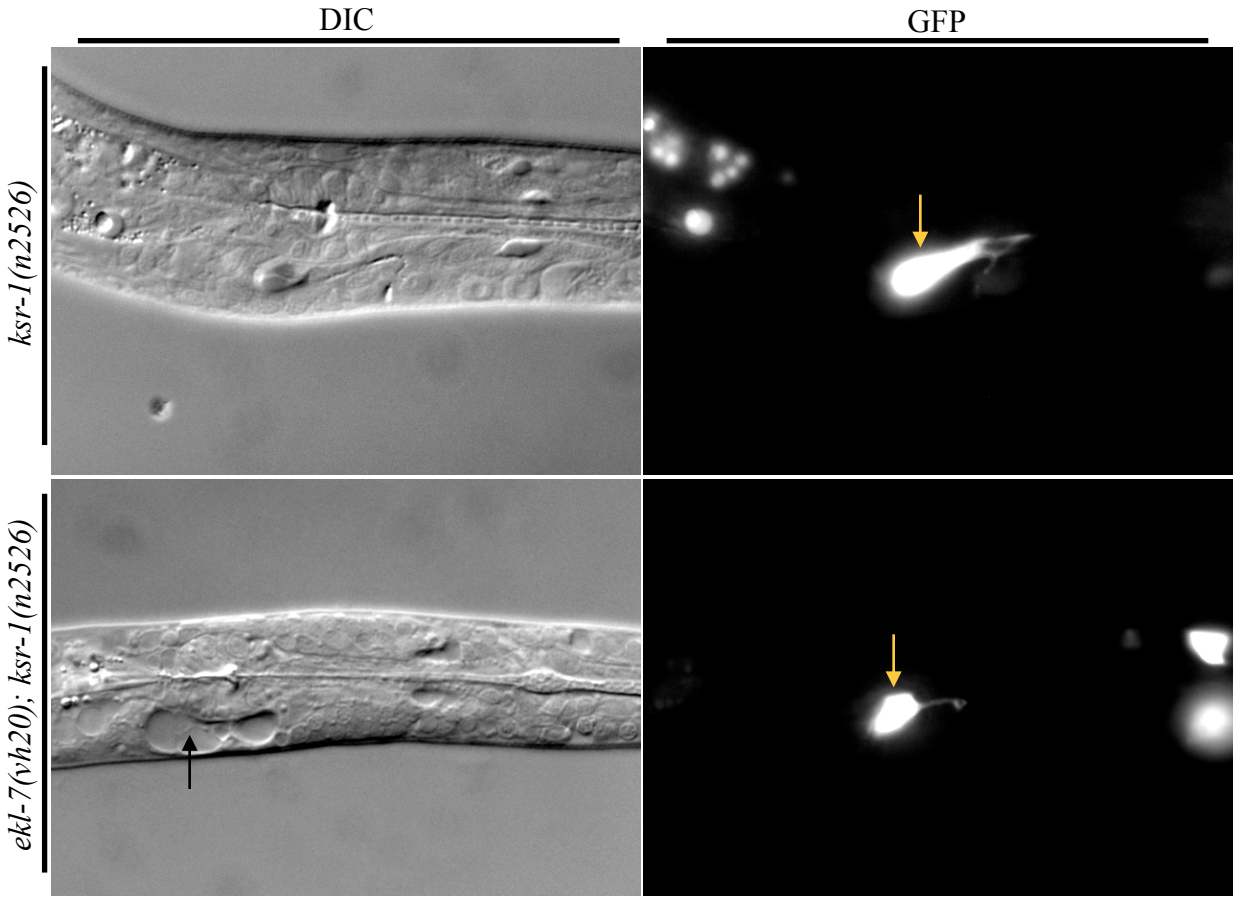

Figure 9: *ksr-1(n2526)* and *ekl-7(vh20); ksr-1(n2526)* mutants always express the *saIs14[plin-48::GFP]* transgene in a single EDC

Mutants at the L1 larval stage carrying the transgene, *saIs14[plin-48::GFP]* were scored for presence or absence of GFP expression in the EDC (yellow arrow). All *ksr-1* animals (*n*=60) and all *ekl-7(vh20); ksr-1(n*=57) animals observed expressed the *lin-48::GFP* reporter in the EDC. Several *ekl-7(vh20); ksr-1* animals showed extensive vacuolarization adjacent to the location of the EDC (black arrow).

Figure 10

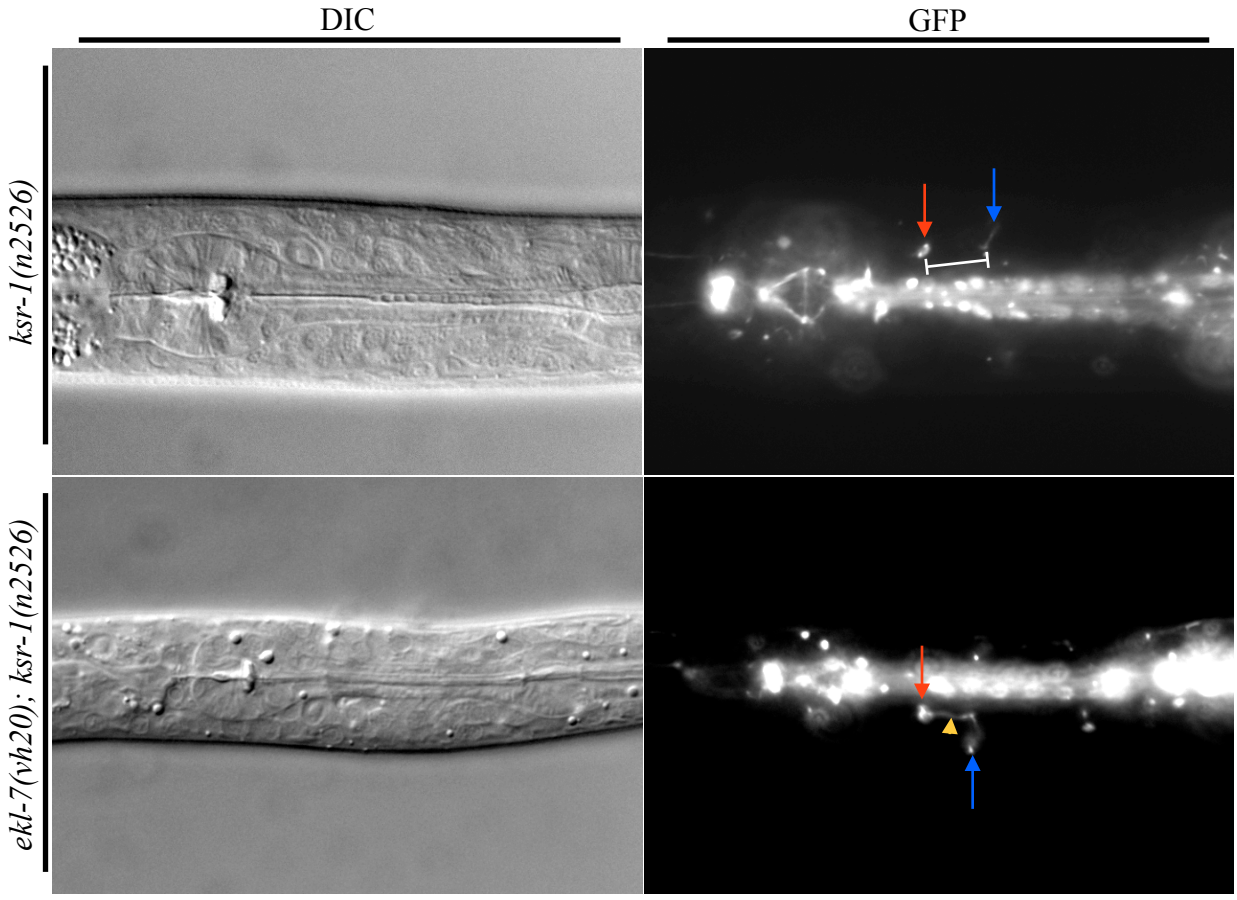

Figure 10: *ekl-7(vh20); ksr-1(n2526)* mutants have EDCs that fail to fuse at the autocellular junction

Excretory ducts were characterized in mutants carrying the transgene, *jcIs1[AJM-1::GFP]*, which marks apical epithelial junctions between the canal cell-EDC epithelial junction (red arrow) and G1 pore autocellular junction (blue arrow). In all *ksr-1* L1 larvae (*n*=52), the autocellular junction always fused (white bracket) as is expected in wild-type. In 16/49 *ekl-7; ksr-1* L1 larvae, the EDC failed to fuse at the autocellular junction (yellow arrowhead) which is typical of mutants with reduced Ras signalling.

Figure 11

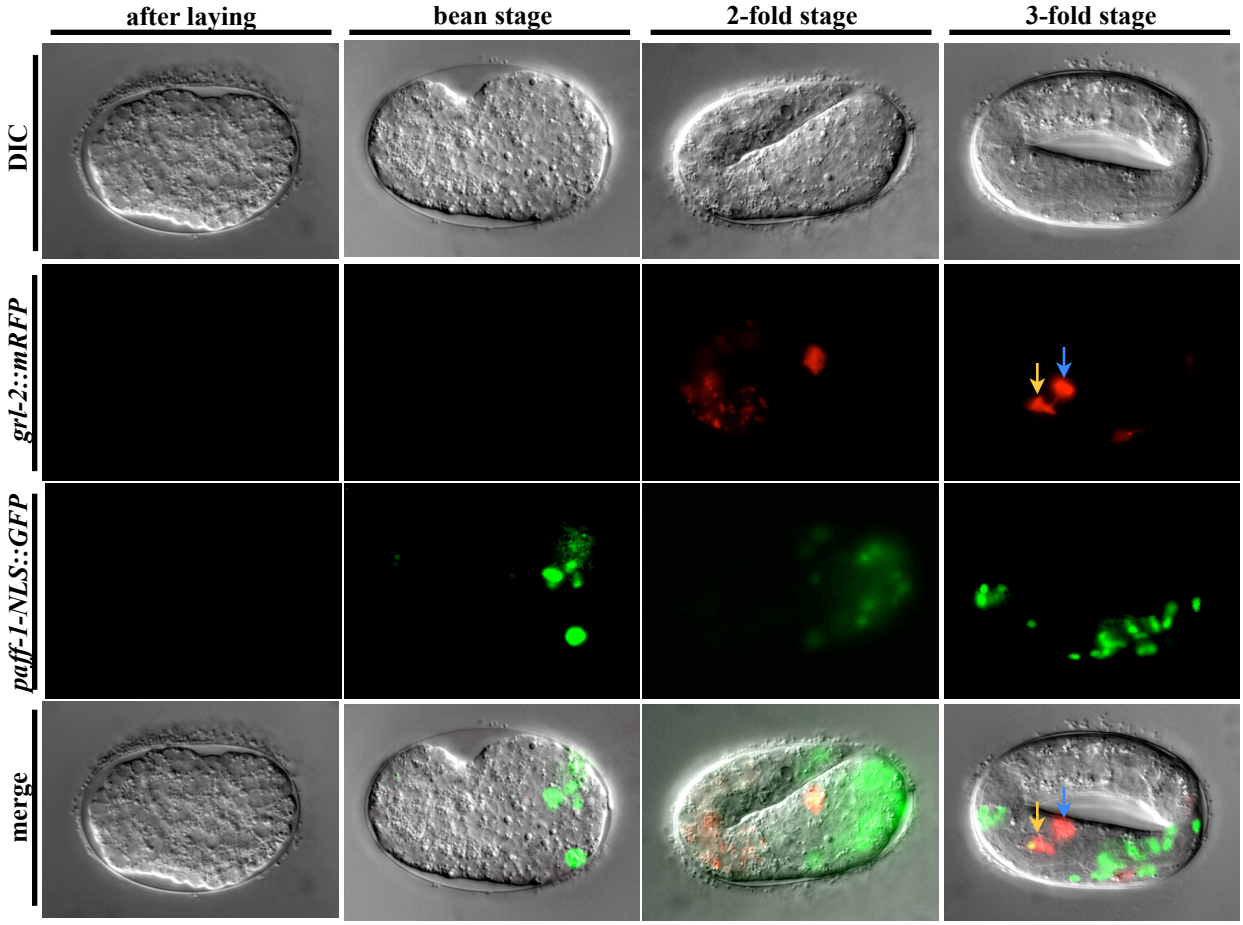

Figure 11: *ksr-1(n2526)* mutant embryos properly express *aff-1* in the EDC
21/22 *ksr-1(n2526)* mutants at the 3-fold stage expressed *aff-1* in the EDC (yellow arrow), distinguishable from the other *grl-2::mRFP*-positive G1 pore cell (blue arrow) by its ventral position. *ksr-1(n2526)* embryos express *aff-1* in the excretory system earlier at the 2-fold stage when the EDC is expected to autofuse.

Figure 12

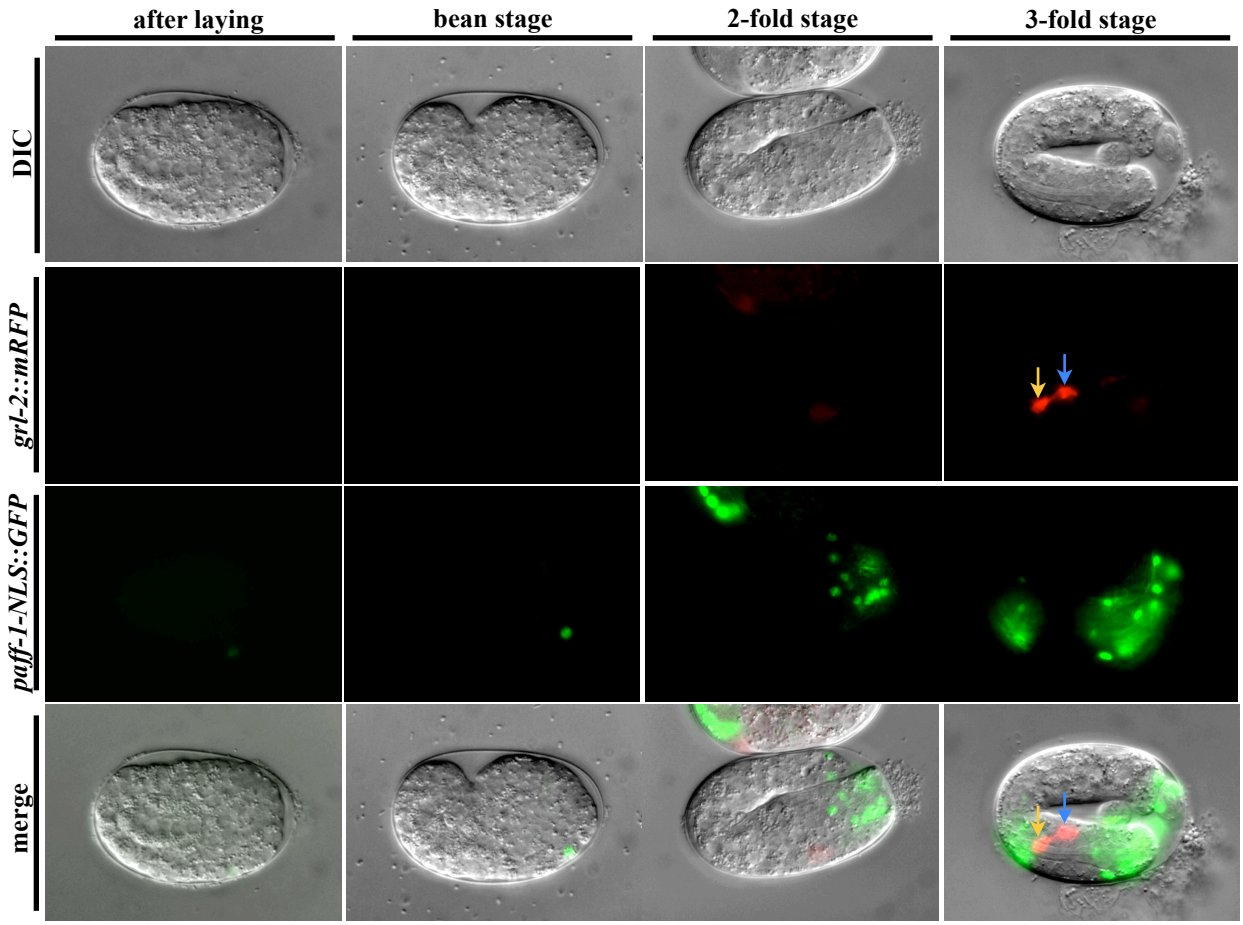

Figure 12: *ekl-7(vh20); ksr-1(n2526)* mutant embryos fail to express *aff-1* in the EDC
6/20 *ekl-7(vh20); ksr-1(n2526)* mutants at the 3-fold stage fail to express *aff-1* in the EDC (yellow arrow), distinguishable from the other *grl-2::mRFP*-positive G1 pore cell (blue arrow) by its ventral position. *aff-1* fails to express in the excretory system of embryos at an earlier 2-fold stage when the EDC is expected to autofuse, and is therefore likely the underlying reason for the EDC autofusion defect detected in *ekl-7(vh20); ksr-1(n2526)* L1 larvae.

Figure 13

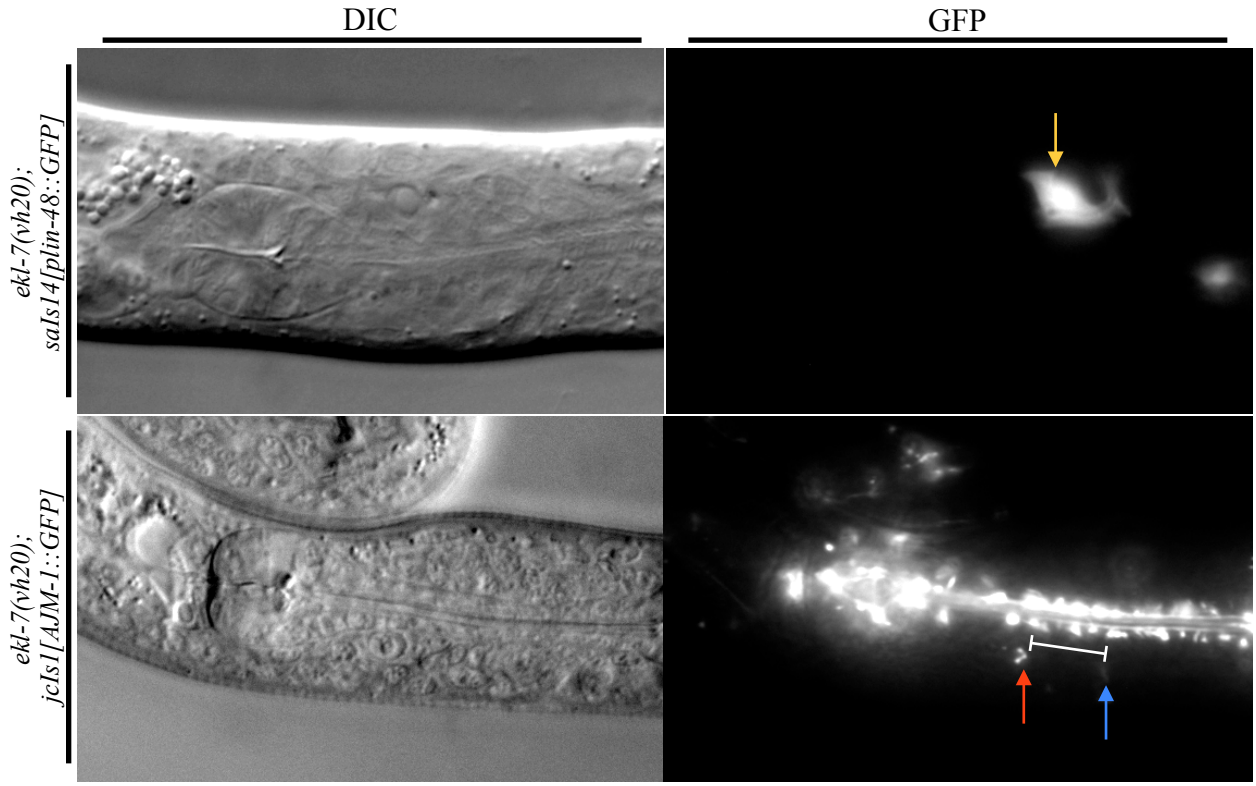

Figure 13: *ekl-7(vh20)* single mutants have wild-type excretory ducts
All *ekl-7(vh20)* L1 larvae carrying the *saIs14[plin-48::GFP]* (*n*=36) and *jcIs1[AJM-1::GFP]* (*n*=44) had wild-type excretory ducts. The *lin-48::GFP* reporter was always expressed in a single EDC (yellow arrow) and the *AJM-1::GFP* reporter showed wild-type expression at the proper epithelial junctions between the canal cell and EDC (red arrow), and G1 pore autocellular junction (blue arrow).

Figure 14

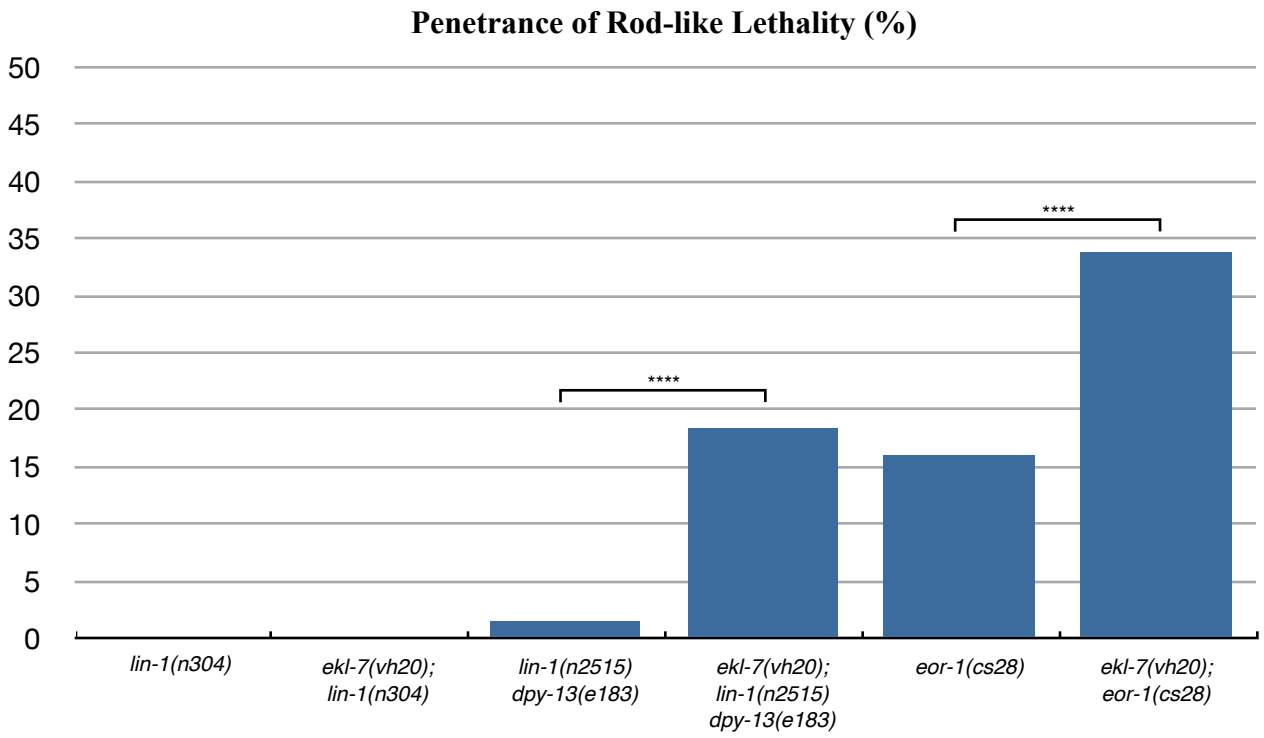

Figure 14: Bringing *ekl-7(vh20)* into either *lin-1(n2515)* or *eor-1(cs28)* mutant backgrounds causes enhancement of rod-like lethality
Significant enhancement of rod-like lethality when *ekl-7(vh20)* is brought into the *lin-1(n2515)* gain-of-function and *eor-1(cs28)* loss-of-function backgrounds suggest that *ekl-7* functions in parallel to both ERK substrates. No rod-like lethality was observed in either *lin-1(n304)* or *ekl-7(vh20); lin-1(n304)* mutants. Statistical significance was analyzed using Fisher's exact test. **** *P<0.0001.*

Figure 15

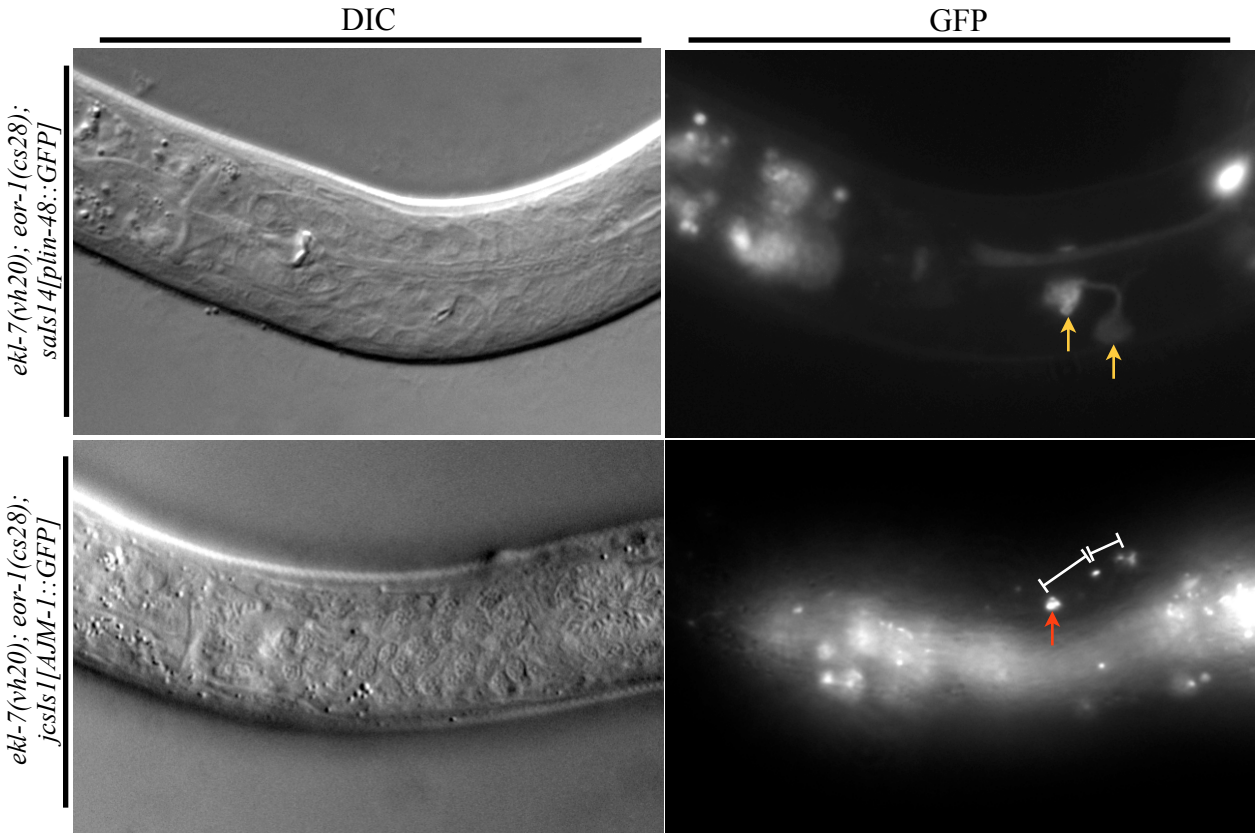

Figure 15: *ekl-7(vh20); eor-1(cs28)* mutants sometimes specify 2 EDCs
4/32 *ekl-7(vh20); eor-1(cs28)* L1 larvae aberrantly expressed *lin-48::GFP* in the G1 pore cell. As well, 3/21 *ekl-7(vh20); eor-1(cs28)* mutants lacked a pore autocellular junction which suggested that a pore-to-EDC transformation had occurred. Yellow arrows indicate the 2 EDCs; white brackets indicate the areas where both EDCs have undergone autofusion between the canal cell (red arrow) and epidermis.

Figure 16

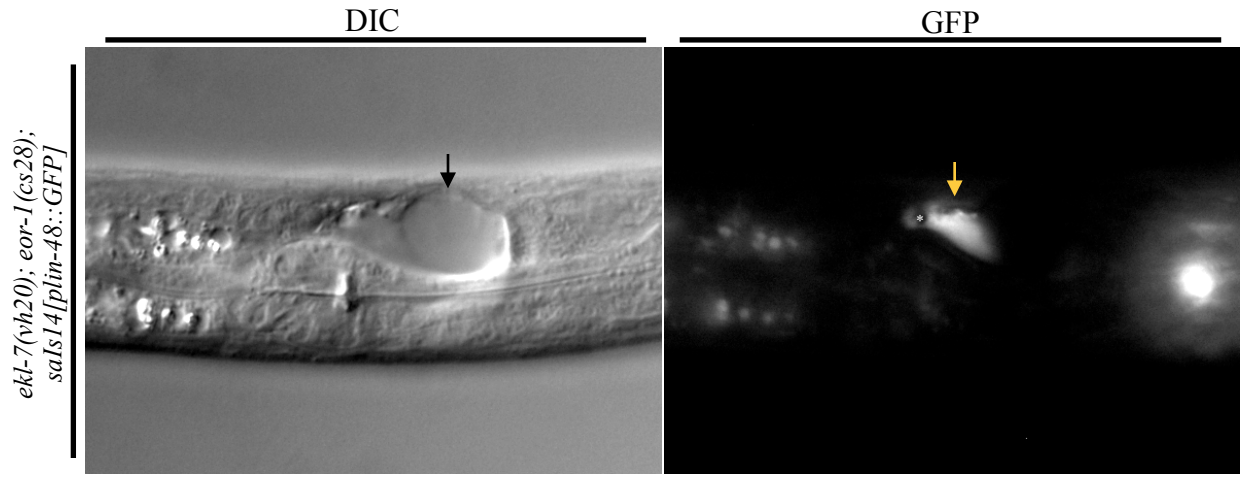

Figure 16: *ekl-7(vh20); eor-1(cs28)* mutants that specify a single EDC commonly have cyst-like formations in the EDC
10/28 *ekl-7(vh20); eor-1(cs28)* L1 larvae that properly expressed the *lin-48::GFP* reporter in a single EDC (yellow arrow) commonly had a cyst-like formation (asterisk) where the duct narrows to joins with the G1 pore cell. Extensive vacuolarization (black arrow) can be seen in the corresponding DIC image indicative of eventual rod-like lethality.

Figure 17

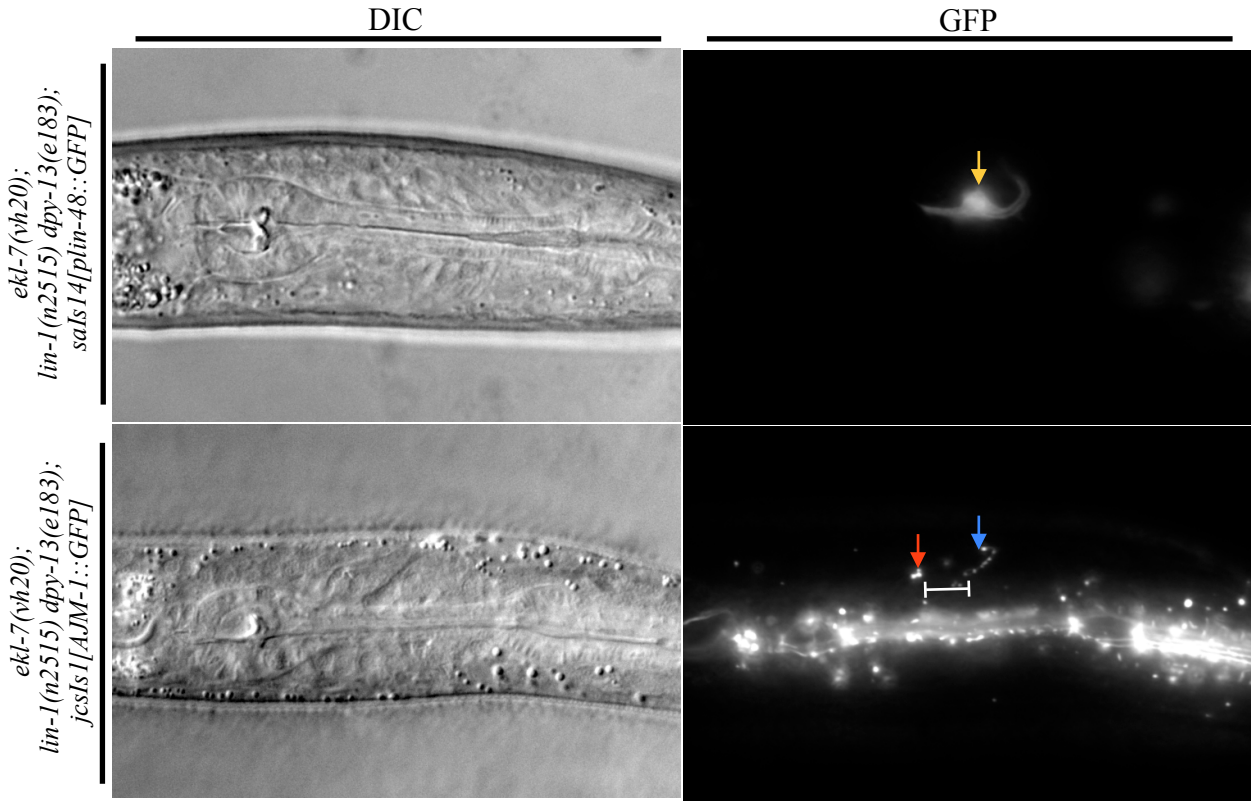

Figure 17: *ekl-7(vh20); lin-1(n2515) dpy-13(e183)* mutants appear to have a defect in the G1 pore autocellular junction

All *ekl-7(vh20); lin-1(n2515) dpy-13(e183)* L1 larvae (*n*=24) carrying the *lin-48::GFP* reporter expressed it in a single EDC. 10/32 of those carrying the *AJM-1::GFP* reporter appeared to have an abnormal autocellular junction where expression along the autocellular junction had a punctate-like appearance.

Figure 18

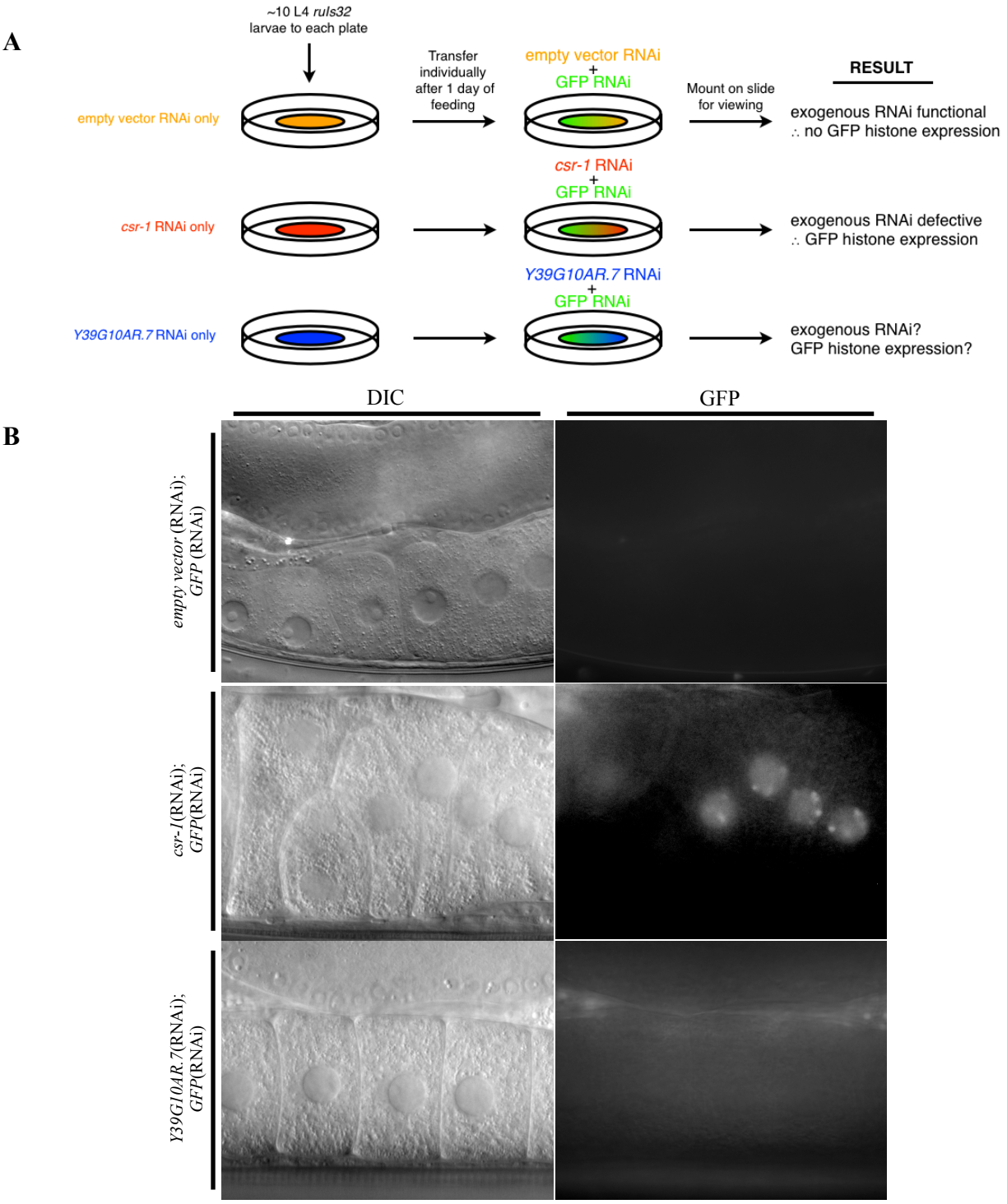

Figure 18: Suppression of *Y39G10AR.7* does not appear to affect exogenous RNAi
[A] RNAi co-suppression assay for exogenous RNAi. [B] *ruIs32[ppie-1::GFP:H2B:pie-1; Punc-119::unc-119(+)]* animals fed *Y39G10AR.7(RNAi)* did not show GFP expression in germline nuclei, indicating exogenous RNAi was unaffected. RNAi against *csr-1*, a germline Argonaute, was used as a positive control.

Figure 19

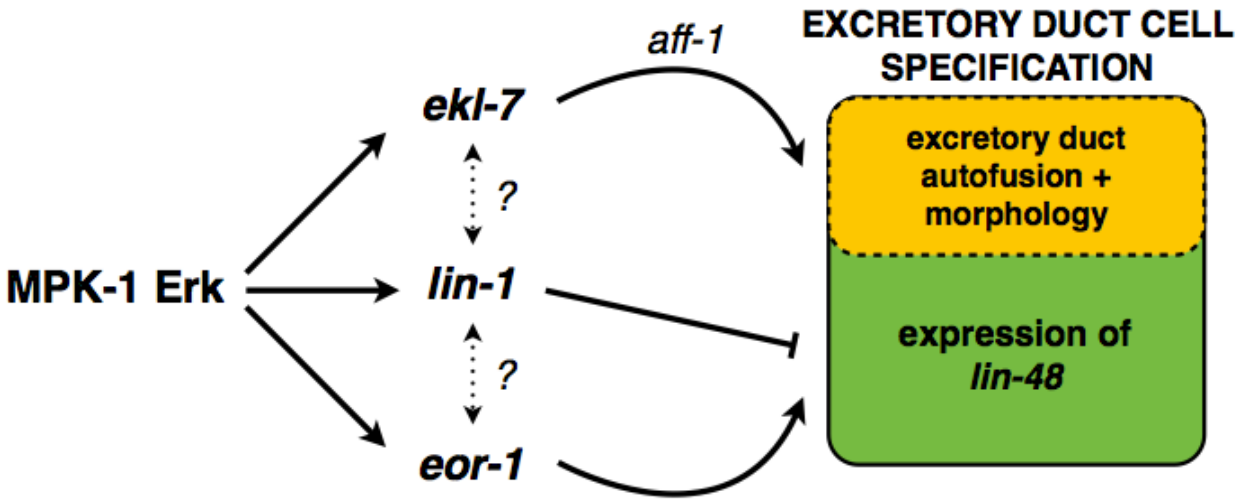

Figure 19: Preliminary model for *ekl-7* function during EDC specification
ekl-7 functions as a positive regulator of EDC fate by regulating *aff-1* expression in the EDC when it autofuses into a seamless toroid early on during embryogenesis. We have shown that the role of *ekl-7* in excretory duct development appears to exclude expression of duct-cell specific *lin-48*. *ekl-7* functions in parallel to ERK substrates *lin-1* and *eor-1,* which also have been previously reported to demonstrate synergistic function with one another during excretory duct development. The nature of these cooperative relationships between downstream ERK substrates is still unclear, but they may function collectively to elicit Ras/MAPK-dependent effects in a tissue-specific manner.

Table 1: *ekl-7(vh20)* is an enhancer of *ksr-1(n2526)* rod-like lethality

Genotype	*n*	Rod-like Lethality (%)
ksr-1(n2526)	1024	3.1
ekl-7(vh20)	920	0.0
ekl-7(vh20); ksr-1(n2526)	1060	35.2****

**** *P<0.0001*, relative to *ksr-1(n2526)*.

Table 2: *ekl-7(vh20); ksr-1(n2526)* mutants have wild-type vulval cell specification

Genotype	*n*	Vulval induction score
ksr-1(n2526)	26	3.00
ekl-7(vh20); ksr-1(n2526)	28	2.98 ns

ns *P>0.05*

Table 3: *vh20* may be a hypomorphic allele of *Y39G10AR.7*

Genotype	*n*	Rod-like Lethality (%)
ksr-1(n2526)*; Y39G10AR.7(RNAi)*	332	22.3
ksr-1(n2526)*; rab-5(RNAi)*	150	0.0
ksr-1(n2526)*; empty vector(RNAi)*	313	2.6
ekl-7(vh20); ksr-1(n2526)*; Y39G10AR.7(RNAi)*	472	41.3****
ekl-7(vh20); ksr-1(n2526)*; rab-5(RNAi)*	286	0.0
ekl-7(vh20); ksr-1(n2526)*; empty vector(RNAi)*	380	28.9

**** *P<0.0001*, relative to empty vector control. *rab-5(RNAi)* was used as a positive feeding control since *rab-5* is an essential small GTPase during early embryogenesis and causes animals to arrest before larval development [91].

Table 4: Mosaically expressing a wild-type copy of *Y39G10AR.7* did not rescue rod-like lethality in *ekl-7(vh20); ksr-1(n2526)* mutants

Genotype	*n*	Rod-like Lethality (%)
ksr-1(n2526)*; vhEx39(Y39G10AR.7)*	86	4.7
ekl-7(vh20); ksr-1(n2526)*; vhEx39(Y39G10AR.7)*	52	36.5
ksr-1(n2526)*; vhEx40(Y39G10AR.7)*	68	2.9
ekl-7(vh20); ksr-1(n2526)*; vhEx40(Y39G10AR.7)*	50	40.0
ksr-1(n2526)*; vhEx41(Y39G10AR.7)*	76	3.9
ekl-7(vh20); ksr-1(n2526)*; vhEx41(Y39G10AR.7)*	54	38.9

Table 5: Oligonucleotide sequences

Primer	Sequence
PCo1	5’ - GAT TCA CGA AGA TCC TCG -3’
PCo2	5’ - GAG CTT CAT CTT GGC ATC TG - 3’
PCo3	5’ - CGA GAT GAC TGT GAA ACG - 3’
PCo4	5’ - TTG AGC CCA GTA TCA ACG - 3’
PCo5	5’ - ACC AAT TAT GGT GCT CCG - 3’
PCo6	5’ - CCT AAT CGT CAT CTT CCT CG - 3’
JHo106	5’ - GAT TAC ACA TGG CAT GGA CG - 3’
JHo107	5’ - CGC TCA TGT TTA GAT TTG GAT TG - 3’
PCo23	5’ - CGA GAT GAC TGT GAA ACG - 3’
PCo24	5’ - GCT GAT GTT TTG GAG ACC - 3’
PCo25	5’ - GAT ACT GGG CTC AAT TAT CC - 3’
PCo26	5’ - CCA GTG AAA AGT TCT TCT CC - 3’
M13_F	5' - GTA AAA CGA CGG CCA GT - 3'
M13_R	5' - GGA AAC AGC TAT GAC CAT G - 3'
L4440_F	5’ - AGC GAG TCA GTG AGC GAG GAA GC - 3’
L4440_R	5’ - GGT TTT CCC AGT CAC GAC GTT G - 3’

List of References

1. Emmons, Scott W. "THE DEVELOPMENT OF SEXUAL DIMORPHISM: STUDIES OF THE *C. ELEGANS* MALE." *Wiley Interdisciplinary Reviews. Developmental Biology*. U.S. National Library of Medicine, 13 May 2014.

2. Brenner, S. "The Genetics of *CAENORHABDITIS ELEGANS*." *Genetics*. U.S. National Library of Medicine.

3. Sulston, J.E., and H.R. Horvitz. "Post-embryonic Cell Lineages of the Nematode, Caenorhabditis Elegans." *Developmental Biology* 56.1 (1977): 110-56.

4. Riddle, Donald L., Thomas Blumenthal, Barbara J. Meyer, and James R. Priess. "C. Elegans II, 2nd Edition." *National Center for Biotechnology Information*. U.S. National Library of Medicine.

5. Wood, William Barry. *The Nematode Caenorhabditis Elegans*. Cold Spring Harbor, NY: Cold Spring Harbor Laboratory, 1988. 1448-452.

6. Sulston, J. E., E. Schierenberg, J. G. White, and J. N. Thomson. "The Embryonic Cell Lineage of the Nematode Caenorhabditis Elegans." *Developmental Biology*, 3 Nov. 1982.

7. Gilbert, Scott F. “Early Development of the Nematode Caenorhabditis Elegans.” *Developmental Biology*. Sunderland, MA: Sinauer Associates, 1988.

8. Bucher, Elizabeth A., and Geraldine Seydoux. "Gastrulation in the Nematode Caenorhabditis Elegans." *Seminars in Developmental Biology* 5.2 (1994): 121-30.

9. Ambros, Victor. "Control of Developmental Timing in Caenorhabditis Elegans." *Current Opinion in Genetics & Development* 10.4 (2000): 428-33.

10. Raizen, David M., John E. Zimmerman, Matthew H. Maycock, Uyen D. Ta, Young-Jai You, Meera V. Sundaram, and Allan I. Pack. "Lethargus Is a Caenorhabditis Elegans Sleep-like State." *Nature* 451.7178 (2008): 569-72.

11. Golden, James W., and Donald L. Riddle. "The Caenorhabditis Elegans Dauer Larva: Developmental Effects of Pheromone, Food, and Temperature." *Developmental Biology* 102.2 (1984): 368-78.

12. Kolch, Walter. "Coordinating ERK/MAPK Signalling through Scaffolds and Inhibitors." *Nature Reviews Molecular Cell Biology Nat Rev Mol Cell Biol* 6.11 (2005): 827-37.

13. Karnoub, Antoine E., and Robert A. Weinberg. "Ras Oncogenes: Split Personalities." *Nature Reviews Molecular Cell Biology Nat Rev Mol Cell Biol* 9.7 (2008): 517-31.

14. Fernandez-Medarde, A., and E. Santos. "Ras in Cancer and Developmental Diseases." *Genes & Cancer* 2.3 (2011): 344-58.

15. Wicker, L. S., B. J. Miller, and Y. Mullen. "Transfer of Autoimmune Diabetes Mellitus with Splenocytes from Nonobese Diabetic (NOD) Mice." *Diabetes* 35.8 (1986): 855-60.

16. Bollag, Gideon, D. Wade Clapp, Shane Shih, Felix Adler, You Yan Zhang, Patricia Thompson, Beverly J. Lange, Melvin H. Freedman, Frank Mccormick, Tyler Jacks, and Kevin Shannon. "Loss of NF1 Results in Activation of the Ras Signaling Pathway and Leads to Aberrant Growth in Haematopoietic Cells." *Nature Genetics Nat Genet* 12.2 (1996): 144-48.

17. Krauss, Gerhard. "Membrane Receptors with Associated Tyrosine Kinase Activity." *Biochemistry of Signal Transduction and Regulation* (2014): 593-630.

18. Hubbard, Stevan R., and W. Todd Miller. "Receptor Tyrosine Kinases: Mechanisms of Activation and Signaling." *Current Opinion in Cell Biology* 19.2 (2007): 117-23.

19. Lemmon, Mark A., and Joseph Schlessinger. "Cell Signaling by Receptor Tyrosine Kinases." *Cell* 141.7 (2010): 1117-134.

20. Lodish, Harvey. "Molecular Biology of the Cell, 4th Edition." *Receptor Tyrosine Kinases and Ras* 18.3 (2002).

21. Lemmon, M. A., J. E. Ladbury, V. Mandiyan, and J. Schleissinger. "Independent Binding of Peptide Ligands to the SH2 and SH3 Domains of Grb2." *Journal of Cell Biology* 13th ser. 269.50 (1994): 31653-1658.

22. Rogge, Ronald D., Chris A. Karlovich, and Utpal Banerjee. "Genetic Dissection of a Neurodevelopmental Pathway: Son of Sevenless Functions Downstream of the Sevenless and EGF Receptor Tyrosine Kinases." *Cell* 64.1 (1991): 39-48.

23. Wan, Paul T.C, Mathew J. Garnett, S.mark Roe, Sharlene Lee, Dan Niculescu-Duvaz, Valerie M. Good, Cancer Genome Project, C.michael Jones, Christopher J. Marshall, Caroline J. Springer, David Barford, and Richard Marais. "Mechanism of Activation of the RAF-ERK Signaling Pathway by Oncogenic Mutations of B-RAF." *Cell* 116.6 (2004): 855-67.

24. Yoon, Seunghee, and Rony Seger. "The Extracellular Signal-regulated Kinase: Multiple Substrates Regulate Diverse Cellular Functions." *Growth Factors* 24.1 (2006): 21-44.

25. Hill, Russell J., and Paul W. Sternberg. "The Gene Lin-3 Encodes an Inductive Signal for Vulval Development in C. Elegans." *Nature* 358.6386 (1992): 470-76.

26. Devore, Dianna L., H.robert Horvitz, and Michael J.stern. "An FGF Receptor Signaling Pathway Is Required for the Normal Cell Migrations of the Sex Myoblasts in C. Elegans Hermaphrodites." *Cell* 83.4 (1995): 611-20.

27. Sasson, I. E. "FGF and PI3 Kinase Signaling Pathways Antagonistically Modulate Sex Muscle Differentiation in C. Elegans." *Development* 131.21 (2004): 5381-392.

28. Bülow, Hannes E., Thomas Boulin, and Oliver Hobert. "Differential Functions of the C. Elegans FGF Receptor in Axon Outgrowth and Maintenance of Axon Position." *Neuron* 42.3 (2004): 367-74.

29. Borland, Christina Z., Jennifer L. Schutzman, and Michael J. Stern. "Fibroblast Growth Factor Signaling InCaenorhabditis Elegans." *Bioessays BioEssays* 23.12 (2001): 1120-130.

30. Meister, Melanie, Ana Tomasovic, Antje Banning, and Ritva Tikkanen. "Mitogen-Activated Protein (MAP) Kinase Scaffolding Proteins: A Recount." *IJMS International Journal of Molecular Sciences* 14.3 (2013): 4854-884.

31. Sacks, D.B. "The Role of Scaffold Proteins in MEK/ERK Signalling." *Biochm. Soc. Trans. Biochemical Society Transactions* 34.5 (2006): 833-36.

32. Kolch, Walter. "Coordinating ERK/MAPK Signalling through Scaffolds and Inhibitors." *Nature Reviews Molecular Cell Biology Nat Rev Mol Cell Biol* 6.11 (2005): 827-37.

33. Good, M. C., J. G. Zalatan, and W. A. Lim. "Scaffold Proteins: Hubs for Controlling the Flow of Cellular Information." *Science* 332.6030 (2011): 680-86.

34. Roy, F. "KSR Is a Scaffold Required for Activation of the ERK/MAPK Module." *Genes & Development* 16.4 (2002): 427-38.

35. Morrison, D.K. “KSR: a MAPK scaffold of the Ras Pathway?” *Journal of Cell Science.* 114.9: 1609-12.

36. Denouel-Galy, A., E.M. Douville, P.H. Warne, C. Papin, D. Laugier, G. Calothy, J. Downward, and A. Eychène. "Murine Ksr Interacts with MEK and Inhibits Ras-induced Transformation." *Current Biology* 8.1 (1998): 46-55.

37. Cacace, A.M., Michaud, N.R., Therrien M., Mathes K., Copeland T., Rubin G.M., and Morrison D.K. “Identification of Constitutive and Ras-Inducible Phosphorylation Sites of KSR: Implications for 14-3-3 Binding, Mitogen-Activated Protein Kinase Binding, and KSR Overexpression.” *Molecular and Cellular Biology* 19.1 (1999): 229-240.

38. Stewart S., Sundaram M., Zhang Y., Lee J., Han M., and Guan K.L. “Kinase suppressor of Ras forms a multiprotein signaling complex and modulates MEK localization.” *Molecular and Cellular Biology* 19.8 (1999): 5523-34.

39. Kornfeld, Kerry, Dennis B. Hom, and H. Robert Horvitz. "The Ksr-1 Gene Encodes a Novel Protein Kinase Involved in Ras-mediated Signaling in C. Elegans." *Cell* 83.6 (1995): 903-13.

40. Ohmachi, Mitsue, Christian E. Rocheleau, Diane Church, Eric Lambie, Tim Schedl, and Meera V. Sundaram. "C. Elegans Ksr-1 and Ksr-2 Have Both Unique and Redundant Functions and Are Required for MPK-1 ERK Phosphorylation." *Current Biology* 12.5 (2002): 427-33.

41. Yochem J., Sundaram M., and Han M. “Ras is required for a limited number of cell fates and not for general proliferation in Caenorhabditis elegans.” *Molecular and Cellular Biology* 17.5 (1997): 2716-22.

42. Liegeois, S., A. Benedetto, G. Michaux, G. Belliard, and M. Labouesse. "Genes Required for Osmoregulation and Apical Secretion in Caenorhabditis Elegans." *Genetics* 175.2 (2007): 709-24.

43. Stone, Craig E., David H. Hall, and Meera V. Sundaram. "Lipocalin Signaling Controls Unicellular Tube Development in the Caenorhabditis Elegans Excretory System." *Developmental Biology* 329.2 (2009): 201-11.

44. Rocheleau, C. E., K. Cullison, K. Huang, Y. Bernstein, A. C. Spilker, and M. V. Sundaram. "The Caenorhabditis Elegans Ekl (Enhancer of Ksr-1 Lethality) Genes Include Putative Components of a Germline Small RNA Pathway." *Genetics* 178.3 (2008): 1431-443.

45. Salser, S. J., C. M. Loer, and C. Kenyon. "Multiple HOM-C Gene Interactions Specify Cell Fates in the Nematode Central Nervous System." *Genes & Development* 7.9 (1993): 1714-724.

46. Kimble, Judith. "Alterations in Cell Lineage following Laser Ablation of Cells in the Somatic Gonad of Caenorhabditis Elegans." *Developmental Biology* 87.2 (1981): 286-300.

47. Sulston, J.E., and J.G. White. "Regulation and Cell Autonomy during Postembryonic Development of Caenorhabditis Elegans." *Developmental Biology* 78.2 (1980): 577-97.

48. Sternberg, Paul W., and Horvitz, H. R. "Pattern Formation during Vulval Development in C. Elegans." *Cell* 44.5 (1986): 761-72.

49. Sternberg, P. W. "DEVELOPMENTAL BIOLOGY: A Pattern of Precision." *Science* 303.5658 (2004): 637-38.

50. Sundaram, Meera V. "Vulval Development: The Battle between Ras and Notch." *Current Biology* 14.8 (2004).

51. Chen, Ning, and Iva Greenwald. "The Lateral Signal for LIN-12/Notch in C. Elegans Vulval Development Comprises Redundant Secreted and Transmembrane DSL Proteins." *Developmental Cell* 6.2 (2004): 183-92.

52. Hajnal, A., C. W. Whitfield, and S. K. Kim. "Inhibition of Caenorhabditis Elegans Vulval Induction by Gap-1 and by Let-23 Receptor Tyrosine kinase." *Genes & Development* 11.20 (1997): 2715-728.

53. Wang, Minqin, and Paul W. Sternberg. "Competence and Commitment of Caenorhabditis Elegans Vulval Precursor Cells." *Developmental Biology* 212.1 (1999): 12-24.

54. Ferguson E. L. and H. R. Horvitz. “Identification and Characterization of 22 Genes That Affect the Vulval Cell Lineages of the Nematode CAENORHABDITIS ELEGANS.” *Genetics* 110.1 (1985): 17-72.

55. Ferguson, E. L., and H. R. Horvitz. "The Multivulva Phenotype of Certain C. Elegans Mutants Results from Defects in Two Functionally Redundant Pathways." *Trends in Genetics* 5 (1989): 363.

56. Nelson, F. Kenneth, and Donald L. Riddle. "Functional Study of The Caenorhabditis Elegans Secretory-Excretory System Using Laser Microsurgery." *J. Exp. Zool. Journal of Experimental Zoology* 231.1 (1984): 45-56.

57. Nelson, F. Kenneth, Patrice S. Albert, and Donald L. Riddle. "Fine Structure of the Caenorhabditis Elegans Secretory-excretory System." *Journal of Ultrastructure Research* 82.2 (1983): 156-71.

58. White, John. *The Nematode Caenorhabditis Elegans*. Cold Spring Harbor, NY: Cold Spring Harbor Laboratory, 1988. 81-122.

59. Mancuso, V. P., J. M. Parry, L. Storer, C. Poggioli, K. C. Q. Nguyen, D. H. Hall, and M. V. Sundaram. "Extracellular Leucine-rich Repeat Proteins Are Required to Organize the Apical Extracellular Matrix and Maintain Epithelial Junction Integrity in C. Elegans." *Development* 139.5 (2012): 979-90.

60. Abdus-Saboor, I., V. P. Mancuso, J. I. Murray, K. Palozola, C. Norris, D. H. Hall, K. Howell, K. Huang, and M. V. Sundaram. "Notch and Ras Promote Sequential Steps of Excretory Tube Development in C. Elegans." *Development* 138.16 (2011): 3545-555.

61. Rasmussen, Jeffrey P., Kathryn English, Jennifer R. Tenlen, and James R. Priess. "Notch Signaling and Morphogenesis of Single-Cell Tubes in the C. Elegans Digestive Tract." *Developmental Cell* 14.4 (2008): 559-69.

62. Sapir, A., Choi J., Leikina E., Avinoam O., Valansi C., Chernomordik L.V., Newman A.P., and Pobilewicz B. "AFF-1, a FOS-1-Regulated Fusogen, Mediates Fusion of the Anchor Cell in C. elegans." *Developmental Cell* 12.5 (2007): 683-98.

63. Mohler, William A., Gidi Shemer, Jacob J. Del Campo, Clari Valansi, Eugene Opoku-Serebuoh, Victoria Scranton, Nirit Assaf, John G. White, and Benjamin Podbilewicz. "The Type I Membrane Protein EFF-1 Is Essential for Developmental Cell Fusion." *Developmental Cell* 2.3 (2002): 355-62.

64. Friedlander-Shani, Lilach, and Benjamin Podbilewicz. "Heterochronic Control of AFF-1-Mediated Cell-to-Cell Fusion in C. Elegans." *Advances in Experimental Medicine and Biology Cell Fusion in Health and Disease* (2011): 5-11.

65. Madhani, Hiten D., and Gerald R. Fink. "The Riddle of MAP Kinase Signaling Specificity." *Trends in Genetics* 14.4 (1998): 151-55.

66. Beitel, G. J., S. Tuck, I. Greenwald, and H. R. Horvitz. "The Caenorhabditis Elegans Gene Lin-1 Encodes an ETS-domain Protein and Defines a Branch of the Vulval Induction Pathway." *Genes & Development* 9.24 (1995): 3149-162.

67. Han, Min, and Paul W. Sternberg. "Let-60, a Gene That Specifies Cell Fates during C. Elegans Vulval Induction, Encodes a Ras Protein." *Cell* 63.5 (1990): 921-31.

68. Tan, Patrick B., Mark R. Lackner, and Stuart K. Kim. "MAP Kinase Signaling Specificity Mediated by the LIN-1 Ets/LIN-31 WH Transcription Factor Complex during C. Elegans Vulval Induction." *Cell* 93.4 (1998): 569-80.

69. Mavrothalassitis, George, and Jacques Ghysdael. "Proteins of the ETS Family with Transcriptional Repressor Activity." *Oncogene* 19.55 (2000): 6524-532.

70. Jacobs D., Beitel G.J., Clark S. G., Horvitz H. R., and Kornfled K. "Gain-of-function mutations in the Caenorhabditis elegans lin-1 ETS gene identify a C-terminal regulatory domain phosphorylated by ERK MAP kinase." *Genetics* 149.4 (1998): 1809-22.

71. Jacobs, D., D. Glossip, H. Xing, A. J. Muslin, and K. Kornfeld. "Multiple Docking Sites on Substrate Proteins Form a Modular System That Mediates Recognition by ERK MAP Kinase." *Genes & Development* 13.2 (1999): 163-75.

72. Fantz, D. A., D. Jacobs, D. Glossip, and K. Kornfeld. "Docking Sites on Substrate Proteins Direct Extracellular Signal-regulated Kinase to Phosphorylate Specific Residues." *Journal of Biological Chemistry* 276.29 (2001): 27256-7265.

73. Rocheleau C. E., Howard R. M., Goldman A. P., Volk M. L., Girard L. J., and Sundaram M. V. “A lin-45 raf Enhancer Screen Identifies eor-1,eor-2 and Unusual Alleles of Ras Pathway Genes in Caenorhabditis elegans.” *Genetics* 161.1 (2002): 121-31.

74. Leight, E. R., J. T. Murphy, D. A. Fantz, D. Pepin, D. L. Schneider, T. M. Ratliff, D. H. Mohammad, M. A. Herman, and K. Kornfeld. "Conversion of the LIN-1 ETS Protein of Caenorhabditis Elegans from a SUMOylated Transcriptional Repressor to a Phosphorylated Transcriptional Activator." *Genetics* 199.3 (2015): 761-75.

75. Tiensuu, Teresa, Morten Krog Larsen, Emma Vernersson, and Simon Tuck. "Lin-1 Has Both Positive and Negative Functions in Specifying Multiple Cell Fates Induced by Ras/ MAP Kinase Signaling in C. Elegans." *Developmental Biology* 286.1 (2005): 338-51.

76. Miller L. M., Hess H. A., Doroquez D. B., and Andrews N. M. “Null mutations in the lin-31 gene indicate two functions during Caenorhabditis elegans vulval development.” *Genetics* 156.4 (2000): 1595-602.

77. Miller, L. M., M. E. Gallegos, B. A. Morisseau, and S. K. Kim. "Lin-31, a Caenorhabditis Elegans HNF-3/fork Head Transcription Factor Homolog, Specifies Three Alternative Cell Fates in Vulval Development." *Genes & Development* 7.6 (1993): 933-47.

78. Howard, R. M. "C. Elegans EOR-1/PLZF and EOR-2 Positively Regulate Ras and Wnt Signaling and Function Redundantly with LIN-25 and the SUR-2 Mediator Component." *Genes & Development* 16.14 (2002): 1815-827.

79. Hoeppner, Daniel J., Mona S. Spector, Thomas M. Ratliff, Jason M. Kinchen, Susan Granat, Shih-Chieh Lin, Satjit S. Bhusri, Barbara Conradt, Michael A. Herman, and Michael O. Hengartner. "Eor-1 and Eor-2 Are Required for Cell-specific Apoptotic Death in C. Elegans." *Developmental Biology* 274.1 (2004): 125-38.

80. Iuchi, S. "Three Classes of C2H2 Zinc Finger Proteins." *CMLS, Cell. Mol. Life Sci. Cellular and Molecular Life Sciences* 58.4 (2001): 625-35.

81. Howell, K., S. Arur, T. Schedl, and M. V. Sundaram. "EOR-2 Is an Obligate Binding Partner of the BTB-Zinc Finger Protein EOR-1 in Caenorhabditis Elegans." *Genetics* 184.4 (2010): 899-913.

82. Cheng, Phil. *"*A forward genetic screen for enhancers of ksr-1 lethality." MA thesis. U of McGill, 2010. *eScholarship@McGill*.

83. Fay, David. "Genetic Mapping and Manipulation: Chapter 7-Making Compound Mutants." *WormBook* (2006)

84. McKim K. S., Peters K., and A. M. Rose. "Two types of sites required for meiotic chromosome pairing in Caenorhabditis elegans." *Genetics* 134.3 (1993): 749-68.

85. Maniatis, Tom, and Robin Reed. "An Extensive Network of Coupling among Gene Expression Machines." *Nature* 416.6880 (2002): 499-506.

86. Berezikov, E. "Homologous Gene Targeting in Caenorhabditis Elegans by Biolistic Transformation." *Nucleic Acids Research* 32.4 (2004)

87. Kamath, R. "Genome-wide RNAi Screening in Caenorhabditis Elegans." *Methods* 30.4 (2003): 313-21.

88. Fischer, S. E. J., Q. Pan, P. C. Breen, Y. Qi, Z. Shi, C. Zhang, and G. Ruvkun. "Multiple Small RNA Pathways Regulate the Silencing of Repeated and Foreign Genes in C. Elegans." *Genes & Development* 27.24 (2013): 2678-695.

89. Montgomery, Taiowa A., Young-Soo Rim, Chi Zhang, Robert H. Dowen, Carolyn M. Phillips, Sylvia E. J. Fischer, and Gary Ruvkun. "PIWI Associated SiRNAs and PiRNAs Specifically Require the Caenorhabditis Elegans HEN1 Ortholog Henn-1." *PLoS Genetics PLoS Genet* 8.4 (2012)

90. Simmer, Femke, Marcel Tijsterman, Susan Parrish, Sandhya P. Koushika, Michael L. Nonet, Andrew Fire, Julie Ahringer, and Ronald H.a PlastERK. "Loss of the Putative RNA-Directed RNA Polymerase RRF-3 Makes C. Elegans Hypersensitive to RNAi." *Current Biology* 12.15 (2002): 1317-319.

91. Hyenne, Vincent, Thierry Tremblay-Boudreault, Ramraj Velmurugan, Barth D. Grant, Dinah Loerke, and Jean-Claude Labbé. "RAB-5 Controls the Cortical Organization and Dynamics of PAR Proteins to Maintain C. Elegans Early Embryonic Polarity." *PLoS ONE* 7.4 (2012)